especially into the lung (29). In this model, NK1.1$^+$ cells and IFN-γ have a critical role in the suppression of pulmonary metastases (30).

A mouse model with s.c.-implanted B16D8 and polyI:C therapy has been established in our laboratory (8). To investigate the function of INAM involved in tumor growth retardation mediated by polyI:C, we challenged WT and *Inam*$^{-/-}$ mice with B16D8 implantation and then treated the mice with i.p. injection of polyI:C. The rate of B16D8 growth retardation was indistinguishable between WT and *Inam*$^{-/-}$ mice (Supplemental Fig. 3), which was largely dependent on the antitumor effect of polyI:C. This result is consistent with the observation that there is no difference in tumoricidal activity against B16D8 between WT and *Inam*$^{-/-}$ mice. To determine the role of INAM in the production of IFN-γ by lung NK cells in response to polyI:C, we isolated leukocytes from the lung at 0, 3, and 6 h after administration of polyI:C to B16F10-injected WT and *Inam*$^{-/-}$ mice and determined the intracellular content of IFN-γ in NK cells (Fig. 5A). After 6 h, NK cells isolated from *Inam*$^{-/-}$ mice produced less IFN-γ than WT NK cells (Fig. 5B). To investigate the function of INAM involved in pulmonary metastases induced by polyI:C, we i.v. challenged WT and *Inam*$^{-/-}$ mice with B16F10 cells and then treated the mice by i.p. injection of polyI:C. After four rounds of polyI:C treatment, we counted tumor foci in the lung. Under unstimulated conditions, there was no difference in the number and size of tumor foci in the lungs between WT and *Inam*$^{-/-}$ mice (Fig. 5C). In WT mice, i.p. injection of polyI:C exerted a significant inhibition in the growth of pulmonary metastases in tumor-bearing mice compared with PBS controls (Fig. 5D). In contrast, the effect of polyI:C therapy for pulmonary metastases was partially abrogated in *Inam*$^{-/-}$ mice. These results demonstrate that INAM plays a critical role in IFN-γ production by lung NK cells in response to polyI:C and unequivocally exhibits antitumor function in polyI:C-based cancer immunotherapy against IFN-γ–sensitive tumors metastasized to the lung.

BMDC confer direct cytotoxic activity on NK cells by stimulation with RNA via INAM-dependent cell–cell contact (16). Then, NK cells kill tumor cells via effectors, such as TRAIL and granzyme B, secondary to upregulation of INAM. However, splenic DCs hardly induce direct NK cytotoxicity as shown in this study. In this study, *Inam*$^{-/-}$ mice studies revealed that DC/Mφ primed NK cells in vivo to induce IFN-γ that was a major effector for NK antimetastatic activity. Thus, taken together with the previous results that BMDCs induce NK cytotoxicity via INAM (16), INAM-involved DC–NK contact induces two arrays of NK tumoricidal activities, killer effector and IFN-γ producer, depending on the properties of DC subsets. The role of INAM in ILC activation will be a matter of future interest in this context.

Discussion

In this study, we provide the first demonstration, to our knowledge, that INAM plays a critical role in the interactions of NK-CD8α$^+$ cDCs and Mφs leading to IFN-γ production from NK cells in vivo. Additionally, we also propose that INAM is a novel target molecule for cancer immunotherapy against IFN-γ–suppressible metastasis.

IFN-γ coordinates a diverse array of cellular programs via STAT1 activation, such as antimicrobial response, anti- or protumor response, production of proinflammatory cytokines, and induction of IRF1 (31). IRF1 activates a large number of secondary response genes, which carry out a range of immunomodulatory functions (32, 33). In secondary lymphoid organs including spleen and lymph nodes, NK cells are a dominant IFN-γ producer responding to polyI:C (5). IFN-γ primes Ag-specific CD4$^+$ and CD8$^+$ T cells and also activates other innate immune cells including Mφs (34–36). The TLR3-dependent IFN-γ signaling pathway is important in protecting the host from pathogenesis induced by Coxsackievirus group B serotype 3 infection, which leads to IFN-γ production from NK cells (37, 38). Hence, IFN-γ

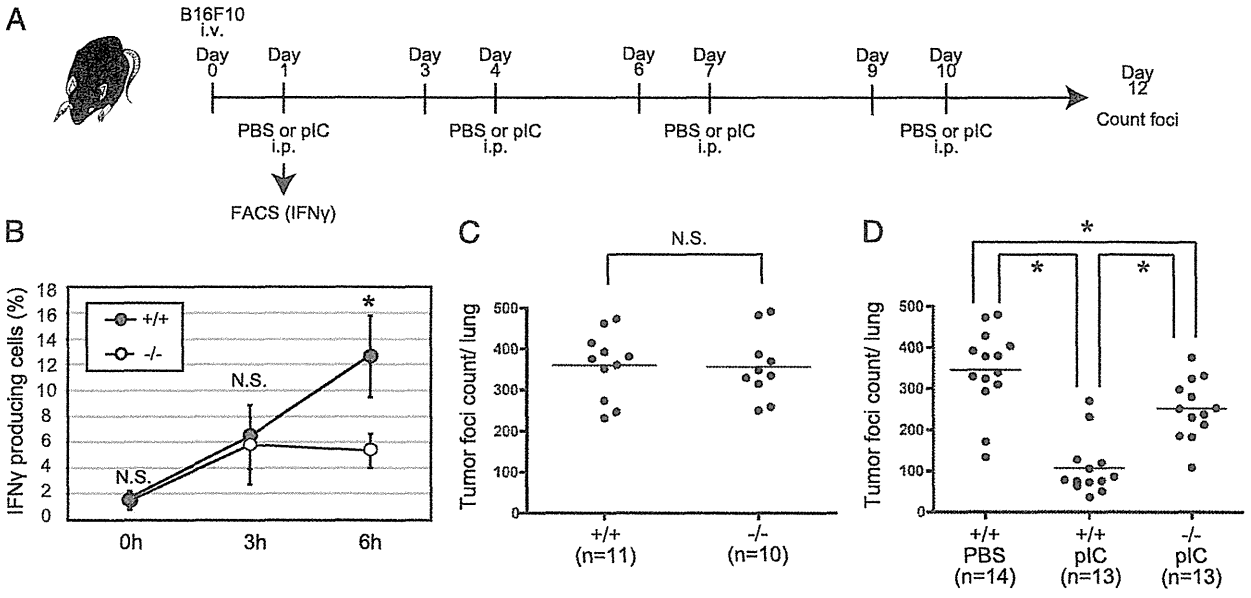

FIGURE 5. Antimetastatic activity of INAM against B16F10 melanoma. (**A**) The time schedule of polyI:C (pIC) treatment. (**B**) Production of IFN-γ by NK cells in the lung. After 24 h, WT and *Inam*$^{-/-}$ mice were i.p. injected with 200 μg polyI:C. Lung leukocytes were isolated and cultured with brefeldin A for an additional 4 h, and analyzed for frequency of NK cells and production of IFN-γ/granzyme B by FACS, gating on CD3ε$^-$/NK1.1$^+$ cells ($n = 3$ or 4). (**C**) Tumor foci counts in the lung of WT (+/+) and *Inam*$^{-/-}$ (−/−) mice under unstimulated conditions at day 12. (**D**) Tumor foci in the lung of WT (+/+) and *Inam*$^{-/-}$ (−/−) mice. WT (+/+) and *Inam*$^{-/-}$ (−/−) mice were i.v. injected with 2×10^5 B16F10 melanoma cells at day 0. At days 1, 4, 7, and 10, WT and *Inam*$^{-/-}$ mice were i.p. injected with 200 μg polyI:C. At day 12, the mice were sacrificed, and lungs were removed and fixed in 10% formalin solution to count surface colonies under a dissection microscope. The data shown are representative of at least two independent experiments. Data are means ± SD of three independent samples. *$p < 0.05$.

derived from NK cells controls innate and adaptive immunity, leading to a Th1 response.

In this study, we show that INAM evokes IFN-γ production by NK cells in the early phase by polyI:C stimulation (Figs. 4B, 5B). In a murine CMV infection model, IFN-γ is induced in NK cells by IL-12 and IL-18 produced by murine CMV–infected CD11b$^+$ cDCs, whereas these cytokines barely evoke any cytotoxic response in NK cells (39). In addition, IFN-γ production from NK cells is induced by anti-CD27 Ab stimulation, but again no cytotoxic response is triggered (24). Therefore, these reports indicate that NK cell cytotoxicity and IFN-γ production are independently controlled by different mechanisms. We found no clear difference between WT and *Inam*$^{-/-}$ mice in expression of these cell surface molecules and cytokines. Hence, the INAM-dependent IFN-γ production from NK cells is based on an as-yet-unknown mechanism(s) acting in a manner independent of these molecules.

CpG DNA is known to induce IFN-γ from NK cells, which is mediated through pDCs. TLR9 in pDCs responds to CpG, and the pDCs liberate IFN-α and TNF-α that participate in the induction of IFN-γ from NK cells (40). We checked induction of the Inam mRNA in spleen after stimulation with CpG in WT and *Inam*$^{-/-}$ mice (Fig. 1E). The levels of *Inam* mRNA as well as numbers of IFN-γ–producing cells were hardly increased in response to i.p. administration of CpG in WT as well as *Inam*$^{-/-}$ mice, suggesting no participation of INAM in CpG-induced NK cell IFN-γ production (data not shown). CpG participates in the activation of the TLR9 pathway in pDCs, but INAM in splenic cDCs and Mφs does not participate in CpG-mediated NK priming. The result is consistent with the fact that polyI:C is an agonist for TLR3 (but not for TLR9 predominantly expressed in pDCs), which is mainly expressed in CD8α$^+$ DCs, especially professional Ag-presenting CD141$^+$ and CD103$^+$ DCs in mice (41).

CD8α$^+$ cDCs directly recognize polyI:C via the TLR3/TICAM-1 pathway and promote IFN-γ production from NK cells in vitro (9). However, previous analysis of *Batf3*$^{-/-}$ mice indicated that absence of CD8α$^+$ cDCs resulted in weak NK cell activation, in agreement with our data (19). We also found that NK cell secretion of IFN-γ was partially decreased in mice depleted of Mφs by injection of clodronate liposomes (Fig. 3E). Notably, expression of INAM by both NK cells and accessory cells is required for early IFN-γ production through NK-CD8α$^+$ cDC and/or NK–Mφ interactions (Fig. 3F, 3G). The physiological role of these accessory cells in NK activation is poorly understood. However, our results indicate that CD8α$^+$ cDCs and Mφs facilitate early secretion of IFN-γ from NK cells in response to polyI:C and INAM plays a critical role in the interaction between NK cells and CD8α$^+$ cDCs and/or Mφs, leading to IFN-γ production.

IFN-γ exhibits both anti- and protumor activities (42). Systemic administration of polyI:C exerted a significant inhibitory effect on the growth of lung metastases in B16F10 melanoma-bearing mice (30, 42). Using this model, a previous study reported that NK1.1$^+$ cells and IFN-γ have a critical role in the protection of lung metastases (30). Previous studies demonstrated that the IFN-γ receptor expressed on host cells, but not on melanoma cells, is important for development of lung metastases (43–45). Hence, lung metastases are prevented by the IFN-γ–inducible immune response following NK cell activation. We show that INAM is involved in the IFN-γ production of lung NK cells in response to polyI:C stimulation and unequivocally exhibits antitumor functions in polyI:C-based cancer immunotherapy against IFN-γ–sensitive tumor foci in the lung (Fig. 5D). Therefore, we propose that INAM is a novel target molecule for cancer immunotherapy against IFN-γ–suppressible metastasis.

Acknowledgments

We thank the members in Seya Laboratory (Hokkaido University). Tumor implant studies were supported by A. Morii-Sakai (Seya Laboratory). Thoughtful discussions with Dr. T. Taniguchi (University of Tokyo) are gratefully acknowledged.

Disclosures

The authors have no financial conflicts of interest.

References

1. Seya, T., J. Kasamatsu, M. Azuma, H. Shime, and M. Matsumoto. 2011. Natural killer cell activation secondary to innate pattern sensing. *J. Innate Immun.* 3: 264–273.
2. Reed, S. G., M. T. Orr, and C. B. Fox. 2013. Key roles of adjuvants in modern vaccines. *Nat. Med.* 19: 1597–1608.
3. Kumar, H., S. Koyama, K. J. Ishii, T. Kawai, and S. Akira. 2008. Cutting edge: cooperation of IPS-1- and TRIF-dependent pathways in poly IC-enhanced antibody production and cytotoxic T cell responses. *J. Immunol.* 180: 683–687.
4. Trumpfheller, C., M. Caskey, G. Nchinda, M. P. Longhi, O. Mizenina, Y. Huang, S. J. Schlesinger, M. Colonna, and R. M. Steinman. 2008. The microbial mimic poly IC induces durable and protective CD4$^+$ T cell immunity together with a dendritic cell targeted vaccine. *Proc. Natl. Acad. Sci. USA* 105: 2574–2579.
5. Longhi, M. P., C. Trumpfheller, J. Idoyaga, M. Caskey, I. Matos, C. Kluger, A. M. Salazar, M. Colonna, and R. M. Steinman. 2009. Dendritic cells require a systemic type I interferon response to mature and induce CD4+ Th1 immunity with poly IC as adjuvant. *J. Exp. Med.* 206: 1589–1602.
6. Talmadge, J. E., J. Adams, H. Phillips, M. Collins, B. Lenz, M. Schneider, E. Schlick, R. Ruffmann, R. H. Wiltrout, and M. A. Chirigos. 1985. Immunomodulatory effects in mice of polyinosinic-polycytidylic acid complexed with poly-L-lysine and carboxymethylcellulose. *Cancer Res.* 45: 1058–1065.
7. Spits, H., D. Artis, M. Colonna, A. Diefenbach, J. P. Di Santo, G. Eberl, S. Koyasu, R. M. Locksley, A. N. McKenzie, R. E. Mebius, et al. 2013. Innate lymphoid cells—a proposal for uniform nomenclature. *Nat. Rev. Immunol.* 13: 145–149.
8. Akazawa, T., T. Ebihara, M. Okuno, Y. Okuda, M. Shingai, K. Tsujimura, T. Takahashi, M. Ikawa, M. Okabe, N. Inoue, et al. 2007. Antitumor NK activation induced by the Toll-like receptor 3-TICAM-1 (TRIF) pathway in myeloid dendritic cells. *Proc. Natl. Acad. Sci. USA* 104: 252–257.
9. Miyake, T., Y. Kumagai, H. Kato, Z. Guo, K. Matsushita, T. Satoh, T. Kawagoe, H. Kumar, M. H. Jang, T. Kawai, et al. 2009. Poly I:C-induced activation of NK cells by CD8 alpha+ dendritic cells via the IPS-1 and TRIF-dependent pathways. *J. Immunol.* 183: 2522–2528.
10. Wulff, S., R. Pries, and B. Wollenberg. 2010. Cytokine release of human NK cells solely triggered with Poly I:C. *Cell. Immunol.* 263: 135–137.
11. Fuchs, A., W. Vermi, J. S. Lee, S. Lonardi, S. Gilfillan, R. D. Newberry, M. Cella, and M. Colonna. 2013. Intraepithelial type 1 innate lymphoid cells are a unique subset of IL-12- and IL-15-responsive IFN-γ-producing cells. *Immunity* 38: 769–781.
12. Matsumoto, M., K. Funami, H. Oshiumi, and T. Seya. 2013. Toll-IL-1-receptor-containing adaptor molecule-1: a signaling adaptor linking innate immunity to adaptive immunity. *Prog. Mol. Biol. Transl. Sci.* 117: 487–510.
13. Shime, H., A. Kojima, A. Maruyama, Y. Saito, H. Oshiumi, M. Matsumoto, and T. Seya. 2014. Myeloid-derived suppressor cells confer tumor-suppressive functions on natural killer cells via polyinosinic:polycytidylic acid treatment in mouse tumor models. *J. Innate Immun.* 6: 293–305.
14. Tu, Z., A. Bozorgzadeh, R. H. Pierce, J. Kurtis, I. N. Crispe, and M. S. Orloff. 2008. TLR-dependent cross talk between human Kupffer cells and NK cells. *J. Exp. Med.* 205: 233–244.
15. Lucas, M., W. Schachterle, K. Oberle, P. Aichele, and A. Diefenbach. 2007. Dendritic cells prime natural killer cells by trans-presenting interleukin 15. *Immunity* 26: 503–517.
16. Ebihara, T., M. Azuma, H. Oshiumi, J. Kasamatsu, K. Iwabuchi, K. Matsumoto, H. Saito, T. Taniguchi, M. Matsumoto, and T. Seya. 2010. Identification of a polyI:C-inducible membrane protein that participates in dendritic cell-mediated natural killer cell activation. *J. Exp. Med.* 207: 2675–2687.
17. Sato, M., H. Suemori, N. Hata, M. Asagiri, K. Ogasawara, K. Nakao, T. Nakaya, M. Katsuki, S. Noguchi, N. Tanaka, and T. Taniguchi. 2000. Distinct and essential roles of transcription factors IRF-3 and IRF-7 in response to viruses for IFN-alpha/beta gene induction. *Immunity* 13: 539–548.
18. Takaki, H., M. Takeda, M. Tahara, M. Shingai, H. Oshiumi, M. Matsumoto, and T. Seya. 2013. The MyD88 pathway in plasmacytoid and CD4+ dendritic cells primarily triggers type I IFN production against measles virus in a mouse infection model. *J. Immunol.* 191: 4740–4747.
19. McCartney, S., W. Vermi, S. Gilfillan, M. Cella, T. L. Murphy, R. D. Schreiber, K. M. Murphy, and M. Colonna. 2009. Distinct and complementary functions of MDA5 and TLR3 in poly(I:C)-mediated activation of mouse NK cells. *J. Exp. Med.* 206: 2967–2976.
20. Hayakawa, Y., N. D. Huntington, S. L. Nutt, and M. J. Smyth. 2006. Functional subsets of mouse natural killer cells. *Immunol. Rev.* 214: 47–55.
21. Edelson, B. T., T. R. Bradstreet, W. Kc, K. Hildner, J. W. Herzog, J. Sim, J. H. Russell, T. L. Murphy, E. R. Unanue, and K. M. Murphy. 2011. Batf3-dependent CD11b(low/-) peripheral dendritic cells are GM-CSF-independent

and are not required for Th cell priming after subcutaneous immunization. *PLoS ONE* 6: e25660.
22. Hildner, K., B. T. Edelson, W. E. Purtha, M. Diamond, H. Matsushita, M. Kohyama, B. Calderon, B. U. Schraml, E. R. Unanue, M. S. Diamond, et al. 2008. Batf3 deficiency reveals a critical role for CD8alpha$^+$ dendritic cells in cytotoxic T cell immunity. *Science* 322: 1097–1100.
23. Tussiwand, R., W. L. Lee, T. L. Murphy, M. Mashayekhi, W. Kc, J. C. Albring, A. T. Satpathy, J. A. Rotondo, B. T. Edelson, N. M. Kretzer, et al. 2012. Compensatory dendritic cell development mediated by BATF-IRF interactions. *Nature* 490: 502–507.
24. Takeda, K., H. Oshima, Y. Hayakawa, H. Akiba, M. Atsuta, T. Kobata, K. Kobayashi, M. Ito, H. Yagita, and K. Okumura. 2000. CD27-mediated activation of murine NK cells. *J. Immunol.* 164: 1741–1745.
25. Ferlazzo, G., M. Pack, D. Thomas, C. Paludan, D. Schmid, T. Strowig, G. Bougras, W. A. Muller, L. Moretta, and C. Münz. 2004. Distinct roles of IL-12 and IL-15 in human natural killer cell activation by dendritic cells from secondary lymphoid organs. *Proc. Natl. Acad. Sci. USA* 101: 16606–16611.
26. Takeda, K., H. Tsutsui, T. Yoshimoto, O. Adachi, N. Yoshida, T. Kishimoto, H. Okamura, K. Nakanishi, and S. Akira. 1998. Defective NK cell activity and Th1 response in IL-18-deficient mice. *Immunity* 8: 383–390.
27. Burke, S., T. Lakshmikanth, F. Colucci, and E. Carbone. 2010. New views on natural killer cell-based immunotherapy for melanoma treatment. *Trends Immunol.* 31: 339–345.
28. Tanaka, H., Y. Mori, H. Ishii, and H. Akedo. 1988. Enhancement of metastatic capacity of fibroblast-tumor cell interaction in mice. *Cancer Res.* 48: 1456–1459.
29. Brown, L. M., D. R. Welch, and S. R. Rannels. 2002. B16F10 melanoma cell colonization of mouse lung is enhanced by partial pneumonectomy. *Clin. Exp. Metastasis* 19: 369–376.
30. Jiang, Q., H. Wei, and Z. Tian. 2008. IFN-producing killer dendritic cells contribute to the inhibitory effect of poly I:C on the progression of murine melanoma. *J. Immunother.* 31: 555–562.
31. Schroder, K., P. J. Hertzog, T. Ravasi, and D. A. Hume. 2004. Interferon-gamma: an overview of signals, mechanisms and functions. *J. Leukoc. Biol.* 75: 163–189.
32. Honda, K., and T. Taniguchi. 2006. IRFs: master regulators of signalling by Toll-like receptors and cytosolic pattern-recognition receptors. *Nat. Rev. Immunol.* 6: 644–658.
33. Miyamoto, M., T. Fujita, Y. Kimura, M. Maruyama, H. Harada, Y. Sudo, T. Miyata, and T. Taniguchi. 1988. Regulated expression of a gene encoding a nuclear factor, IRF-1, that specifically binds to IFN-beta gene regulatory elements. *Cell* 54: 903–913.
34. O'Sullivan, T., R. Saddawi-Konefka, W. Vermi, C. M. Koebel, C. Arthur, J. M. White, R. Uppaluri, D. M. Andrews, S. F. Ngiow, M. W. L. Teng, et al. 2012. Cancer immunoediting by the innate immune system in the absence of adaptive immunity. *J. Exp. Med.* 209: 1869–1882.
35. Mailliard, R. B., Y. I. Son, R. Redlinger, P. T. Coates, A. Giermasz, P. A. Morel, W. J. Storkus, and P. Kalinski. 2003. Dendritic cells mediate NK cell help for Th1 and CTL responses: two-signal requirement for the induction of NK cell helper function. *J. Immunol.* 171: 2366–2373.
36. Martín-Fontecha, A., L. L. Thomsen, S. Brett, C. Gerard, M. Lipp, A. Lanzavecchia, and F. Sallusto. 2004. Induced recruitment of NK cells to lymph nodes provides IFN-gamma for T(H)1 priming. *Nat. Immunol.* 5: 1260–1265.
37. Hühn, M. H., M. Hultcrantz, K. Lind, H. G. Ljunggren, K. J. Malmberg, and M. Flodström-Tullberg. 2008. IFN-gamma production dominates the early human natural killer cell response to Coxsackievirus infection. *Cell. Microbiol.* 10: 426–436.
38. Negishi, H., T. Osawa, K. Ogami, X. Ouyang, S. Sakaguchi, R. Koshiba, H. Yanai, Y. Seko, H. Shitara, K. Bishop, et al. 2008. A critical link between Toll-like receptor 3 and type II interferon signaling pathways in antiviral innate immunity. *Proc. Natl. Acad. Sci. USA* 105: 20446–20451.
39. Andoniou, C. E., S. L. H. van Dommelen, V. Voigt, D. M. Andrews, G. Brizard, C. Asselin-Paturel, T. Delale, K. J. Stacey, G. Trinchieri, and M. A. Degli-Esposti. 2005. Interaction between conventional dendritic cells and natural killer cells is integral to the activation of effective antiviral immunity. *Nat. Immunol.* 6: 1011–1019.
40. Marshall, J. D., D. S. Heeke, C. Abbate, P. Yee, and G. Van Nest. 2006. Induction of interferon-gamma from natural killer cells by immunostimulatory CpG DNA is mediated through plasmacytoid-dendritic-cell-produced interferon-alpha and tumour necrosis factor-alpha. *Immunology* 117: 38–46.
41. Jongbloed, S. L., A. J. Kassianos, K. J. McDonald, G. J. Clark, X. Ju, C. E. Angel, C. J. Chen, P. R. Dunbar, R. B. Wadley, V. Jeet, et al. 2010. Human CD141+ (BDCA-3)+ dendritic cells (DCs) represent a unique myeloid DC subset that cross-presents necrotic cell antigens. *J. Exp. Med.* 207: 1247–1260.
42. Zaidi, M. R., and G. Merlino. 2011. The two faces of interferon-γ in cancer. *Clin. Cancer Res.* 17: 6118–6124.
43. Forte, G., A. Rega, S. Morello, A. Luciano, C. Arra, A. Pinto, and R. Sorrentino. 2012. Polyinosinic-polycytidylic acid limits tumor outgrowth in a mouse model of metastatic lung cancer. *J. Immunol.* 188: 5357–5364.
44. Takeda, K., M. Nakayama, M. Sakaki, Y. Hayakawa, M. Imawari, K. Ogasawara, K. Okumura, and M. J. Smyth. 2011. IFN-γ production by lung NK cells is critical for the natural resistance to pulmonary metastasis of B16 melanoma in mice. *J. Leukoc. Biol.* 90: 777–785.
45. Kakuta, S., Y. Tagawa, S. Shibata, M. Nanno, and Y. Iwakura. 2002. Inhibition of B16 melanoma experimental metastasis by interferon-gamma through direct inhibition of cell proliferation and activation of antitumour host mechanisms. *Immunology* 105: 92–100.

Research Article

Journal of Innate Immunity

J Innate Immun 2015;7:47–58
DOI: 10.1159/000365113

Received: March 14, 2014
Accepted after revision: June 9, 2014
Published online: August 8, 2014

A MAVS/TICAM-1-Independent Interferon-Inducing Pathway Contributes to Regulation of Hepatitis B Virus Replication in the Mouse Hydrodynamic Injection Model

Chean Ring Leong[a] Hiroyuki Oshiumi[a] Masaaki Okamoto[a] Masahiro Azuma[a]
Hiromi Takaki[a] Misako Matsumoto[a] Kazuaki Chayama[b] Tsukasa Seya[a]

[a]Department of Microbiology and Immunology, Graduate School of Medicine, Hokkaido University, Sapporo, and
[b]Department of Gastroenterology and Metabolism, Applied Life Sciences, Institute of Biomedical and Health Sciences, Hiroshima University, Hiroshima, Japan

Key Words
Type I interferon · Hepatitis B virus regulation · Toll/IL-1R homology domain-containing adaptor molecule 1 · Mitochondrial antiviral signaling protein · Pathogen-associated molecular patterns

Abstract
Toll-like receptors (TLRs) and cytoplasmic RNA sensors have been reported to be involved in the regulation of hepatitis B virus (HBV) replication, but remain controversial due to the lack of a natural infectious model. Our current study sets out to characterize aspects of the role of the innate immune system in eliminating HBV using hydrodynamic-based injection of HBV replicative plasmid and knockout mice deficient in specific pathways of the innate system. The evidence indicated that viral replication was not affected by MAVS or TICAM-1 knockout, but absence of interferon regulatory factor 3 (IRF-3) and IRF-7 transcription factors, as well as the interferon (IFN) receptor, had an adverse effect on the inhibition of HBV replication, demonstrating the dispensability of MAVS and TICAM-1 pathways in the early innate response against HBV. *Myd88*$^{-/-}$ mice did not have a significant increase in the initial viremia, but substantial viral antigen persisted in the mice sera, a response similar to *Rag2*$^{-/-}$ mice, suggesting that the MyD88-dependent pathway participated in evoking an adaptive immune response against the clearance of intrahepatic HBV. Taken together, we show that the RNA-sensing pathways do not participate in the regulation of HBV replication in a mouse model; meanwhile MyD88 is implicated in the HBV clearance.

Introduction

Hepatitis B virus (HBV) is a noncytopathic human DNA (hepadna) virus that infects hepatocytes causing acute and chronic hepatitis [1]. More than 360 million people are chronically infected with HBV worldwide. Although less than 5% of HBV-infected patients develop persistent infections that progress to liver cirrhosis and hepatocellular carcinoma, HBV causes about 20% of hepatocellular carcinoma deaths [2]. The adaptive immune response is widely acknowledged as pivotal in the defense against HBV. However, the role of innate immunity during HBV infection remains controversial since analysis in patients at the early stage of infection is unfeasible. In ad-

Dr. Tsukasa Seya
Department of Microbiology and Immunology
Graduate School of Medicine, Hokkaido University
Kita-15, Nishi-7, Kita-ku, Sapporo 060-8638 (Japan)
E-Mail seya-tu@pop.med.hokudai.ac.jp

dition, no reliable cell-based in vitro infection system or convenient animal model is available.

During HBV infection, the HBV genome is delivered into the nucleus. Infection is defined by the formation of covalently closed circular DNA. Following formation of covalently closed circular DNA, viral mRNA and pregenomic RNA are transcribed [3, 4]. The pregenomic RNA is subsequently converted to a partially double-stranded genome by the viral DNA polymerase. Unlike other DNA viruses, HBV uses an RNA proviral intermediate that must be copied back into DNA for replication. Although these replication steps are sequestered in the nucleus of infected cells, cytoplasmic DNA/RNA sensors are reported to affect the efficacy of HBV replication [5, 6]. The association between cytoplasmic pattern recognition receptors and the dynamics of the HBV life cycle in HBV-infected cells needs to be clarified.

Viral RNA is sensed by the innate immune system by either Toll-like receptor 3 (TLR3) or cytoplasmic sensors such as retinoic acid-inducible gene-I (RIG-I) and melanoma differentiation-associated gene 5 (MDA5). RIG-I and MDA5 mainly participate in type I interferon (IFN) induction in conjunction with the adaptor molecule, mitochondrial antiviral signaling protein (MAVS; also called IPS-1, Cardif, or VISA) [7–9]. The Toll/IL-1R homology domain-containing adaptor molecule 1 (TICAM-1; also called TRIF) is the adaptor of TLR3, which senses viral RNA on the endosomal membrane [8–10]. Several DNA sensors, most of which signal through STING for type I IFN induction, have been reported in recent years [11]. A few reports have also mentioned that MAVS participates in DNA sensing in certain human cells whereby poly-dA/dT DNA is found to signal via RIG-I. Later, it was also shown that poly-dA/dT serves as a template for RNA polymerase III to make RIG-I ligands [12–14]. Nevertheless, this hypothesis is unresolved in mouse cells. Once stimulated by the viral DNA/RNA, these adaptor proteins activate IFN regulatory factor (IRF)-3 and IRF-7, which induce type I IFN production [7–9]. These pattern recognition receptor-mediated early innate immune responses are crucial in controlling viral replication and spread before the initiation of more specific and powerful adaptive immune responses [8, 9, 15].

Despite numerous studies on HBV pathogenesis, the putative molecular patterns of HBV that trigger cellular responses remain unknown. A few reports have suggested that the antiviral response against HBV is mediated by the RIG-I/MAVS pathway in the cytosol and its activation is blocked by HBV polymerase in infected cells [16–18]. However, no definitive evidence in vivo is available because analysis on the gene expression and effectors required for elimination of the replicative template has been especially difficult. Since viral clearance is a multifaceted process, we hydrodynamically injected a naked HBV plasmid DNA into wild-type (WT) and gene-disrupted mice deficient in TICAM-1, MAVS, TICAM-1/MAVS, IRF-3/IRF-7, IFNAR, MyD88, or RAG2 to identify and characterize the immunological events for HBV clearance. With the availability of various gene-disrupted mice, our study allows the identification of pathways crucial for the clearance of HBV.

Materials and Methods

Animal Studies

All mice were backcrossed with C57BL/6 mice more than seven times before use. *Ticam-1*$^{-/-}$ [19] and *Mavs*$^{-/-}$ [20] mice were generated in our laboratory as described previously, while *Ticam-1*$^{-/-}$ *Mavs*$^{-/-}$ mice were generated by crossing *Ticam-1*$^{-/-}$ mice with *Mavs*$^{-/-}$ mice. *Irf-3*$^{-/-}$/*Irf-7*$^{-/-}$ and *Ifnar*$^{-/-}$ mice were kindly provided by T. Taniguchi (University of Tokyo, Tokyo, Japan). *Myd88*$^{-/-}$ mice were provided by Drs. K. Takeda and S. Akira (Osaka University, Osaka, Japan). *Rag2*$^{-/-}$ mice were kindly provided by Dr. N. Ishii (Tohoku University, Sendai, Japan). Female C57BL/6J mice were purchased from CLEA Japan (Tokyo) and used at 7–9 weeks of age. All mice were maintained under specific pathogen-free conditions in the animal facility at Hokkaido University Graduate School of Medicine (Sapporo, Japan). Animal experiments were performed according to the guidelines set by the Animal Safety Center, Japan.

Hydrodynamic Transfection of Mice with HBV1.4 Plasmid

The pTER1.4xHBV plasmid containing 1.4-genome length sequences of HBV that were previously shown to produce a similar sedimentation in sucrose density gradient centrifugation to HBV extracted from the serum of carriers [21] was used in this study. A total of 50 μg of the plasmid was injected into the tail vein of 7- to 9-week-old mice in a volume of 2.0 ml of TransIT-QR hydrodynamic delivery solution (Mirus, USA). The total volume was delivered within 3–8 s. Plasmid DNA was prepared by using an Endo-Free plasmid system (Qiagen, Germany) according to the manufacturer's instructions.

Quantification of HBV DNA by Real-Time PCR

To determine the HBV DNA in the serum, 30 μl of each serum sample was pretreated with 20 units of DNase I (Roche, Germany) at 37°C overnight. The encapsidated viral DNA was extracted with the SMITEST kit (Genome Science Laboratories, Tokyo, Japan) following the manufacturer's instructions and dissolved in 20 μl of TE-buffer. The purified viral genome was quantified by real-time PCR using the SYBR green master mix (Life Technologies, USA) and the HBV-DNA-F/R primer (see suppl. table 1 for primer sequences; for all online suppl. material, see www.karger.com/doi/10.1159/000365113). Amplification conditions included initial denaturation at 95°C for 10 min, followed by 45 cycles of

denaturation at 95°C for 15 s, annealing at 58°C for 5 s, and extension at 72°C for 6 s. The lower detection limit of this assay is 1,000 copies.

Immunohistochemical Staining for HBV Core Antigen

For immunohistochemical staining of the HBV core antigen (HBcAg), mouse livers were fixed with 4% paraformaldehyde overnight, cryoprotected in 30% sucrose, and sectioned at a thickness of 10 μm using Leica cryostat and mounted on Superfrost glass slides. Sections were incubated with the primary antibody (anticore polyclonal rabbit antibody, DAKO) overnight, followed by incubation with an immunoperoxidase technique involving avidin-biotin peroxidase complexes (Vectastain ABC kit; Vector Laboratories, Burlingame, Calif., USA) according to a method reported previously [22].

HBV Surface Antigen Antigenemia

Mice were bled on the days mentioned after injection of pTER-1.4xHBV and serum was isolated by centrifugation. Concentration of HBV surface antigen (HBsAg) in the serum was quantified by sandwich ELISA in commercial ELISA kits following the manufacturer's protocol (XpressBio, USA). The reporting unit is the signal/cutoff ratio of the 1,000-fold diluted serum at an O.D. of 450 nm.

Southern Blotting to Detect Intracapsid HBV DNA

Viral DNA was isolated from intracellular viral capsids and detected with a specific DIG-labeled probe as described previously [21]. In brief, to isolate the viral DNA, mouse livers were homogenized and subjected to overnight sodium dodecyl sulfate-proteinase K digestion followed by phenol extraction and ethanol precipitation. Twenty micrograms of the isolated DNA was separated in 1% agarose gel, transferred onto Immobilon-Ny+ charged nylon membrane (Milipore), and detected with a full-length HBV-DNA probe labeled by the DIG DNA labeling and detection kit (Roche Diagnostics, Basel, Switzerland) according to the instructions provided by the manufacturer.

Anti-HBs Antibody ELISA

IgG antibodies specific for HBsAg were detected by ELISA as described previously [23] with slight modification. A 96-well plate was coated with antigen of HBs in carbonate buffer and followed by blocking of 2% BSA. Plasma samples were diluted 5× and then incubated in the antigen-coated wells for 3 h at room temperature. A horseradish peroxidase-conjugated goat anti-mouse IgGγ (Southern Biotechnology, USA) and TMB were used to develop the signal. Plates were read at 450 nm. Normal mouse plasma was used to generate cutoff values. The antibody titers are reported as the reciprocal of A_{450} (sample)/A_{450} (2.1' normal mouse average) at which samples with a value >1 were considered to have scored positive.

Quantitative HBV or Cytokines mRNA in the Organs

Each organ was extracted from the mice on the days mentioned after hydrodynamic injection of the HBV plasmid. Total RNA of the organs was isolated with TRIzol according to the manufacturer's protocol. Using 0.5–1 μg of total RNA as a template, cDNA was obtained using a high-capacity cDNA transcription kit (Applied Biosystems) according to manufacturer's instructions. qPCR was performed using a Step One real-time PCR system (Applied Biosystems). The expression of cytokine mRNA was normalized to that of β-actin mRNA in each organ, and the fold increase was determined by dividing the expression in each sample by that of the mice receiving the control plasmid. The primer sequences are described in online supplementary table 1.

Quantitative cGAS, STING, and MAVS Expression in Cell Lines

Total RNA was isolated from L929 cells, RAW264.7 cells, immortalized mouse hepatocytes, Huh7 cells, and HepG2 cells with TRIzol according to the manufacturer's protocol. Using 0.5–1 μg of total RNA as a template, cDNA was obtained using a high-capacity cDNA transcription kit (Applied Biosystems) according to manufacturer's instruction. qPCR was performed using a Step One real-time PCR system (Applied Biosystems). The expression of each targeted mRNA was normalized to that of β-actin mRNA in each sample and shown as a relative expression. The primer sequences are described in online supplementary table S1.

Reporter Gene Assay

To prepare the HBV RNA, immortalized mouse hepatocytes previously established in our laboratory [24] were transfected with either control plasmid or pTER1.4xHBV. Total RNA containing the HBV RNA was isolated after 12 h and confirmed with RT-PCR, while the RNA transfected with only control plasmid was used as a control. The isolated RNA was later used as stimuli for the reporter gene assay of IFN-β. Briefly, the immortalized hepatocytes were again transfected with the reporter plasmids. After 16 h, the immortalized hepatocytes were transfected with the stimuli including PIC, a control plasmid, HBV RNA, and pTER1.4xHBV using FuGENE HD (Roche). Cells were lysed at the time point mentioned using a passive lysis buffer, and Firefly and Renilla luciferase activities were determined using a dual-luciferase reporter assay kit. Firefly luciferase activity was normalized by Renilla luciferase activity and was expressed as the fold stimulation relative to activity in nonstimulated cells.

Statistical Analysis

The statistical significance of the obtained data in this study was analyzed using a two-tail unpaired t test and $p < 0.05$ was regarded as statistically significant.

Results

MAVS and TICAM-1 Are Dispensable in Suppressing HBV Replication

We hydrodynamically transfected replication-competent HBV DNA into *Mavs*$^{-/-}$ or *Ticam-1*$^{-/-}$ and *Mavs*$^{-/-}$/*Ticam-1*$^{-/-}$ mice to access the role of these viral RNA-sensing pathways in response to HBV. Serum HBsAg and HBV-DNA levels were monitored regularly as surrogate markers of HBV replication in vivo. WT mice displayed acute self-limiting hepatitis with peak HBs antigenemia on day 4 after DNA injection (fig. 1a–c). Subsequently, HBsAg in sera decreased and terminated by day 11. *Mavs*$^{-/-}$ and *Ticam-1*$^{-/-}$ mice displayed HBsAg clearance

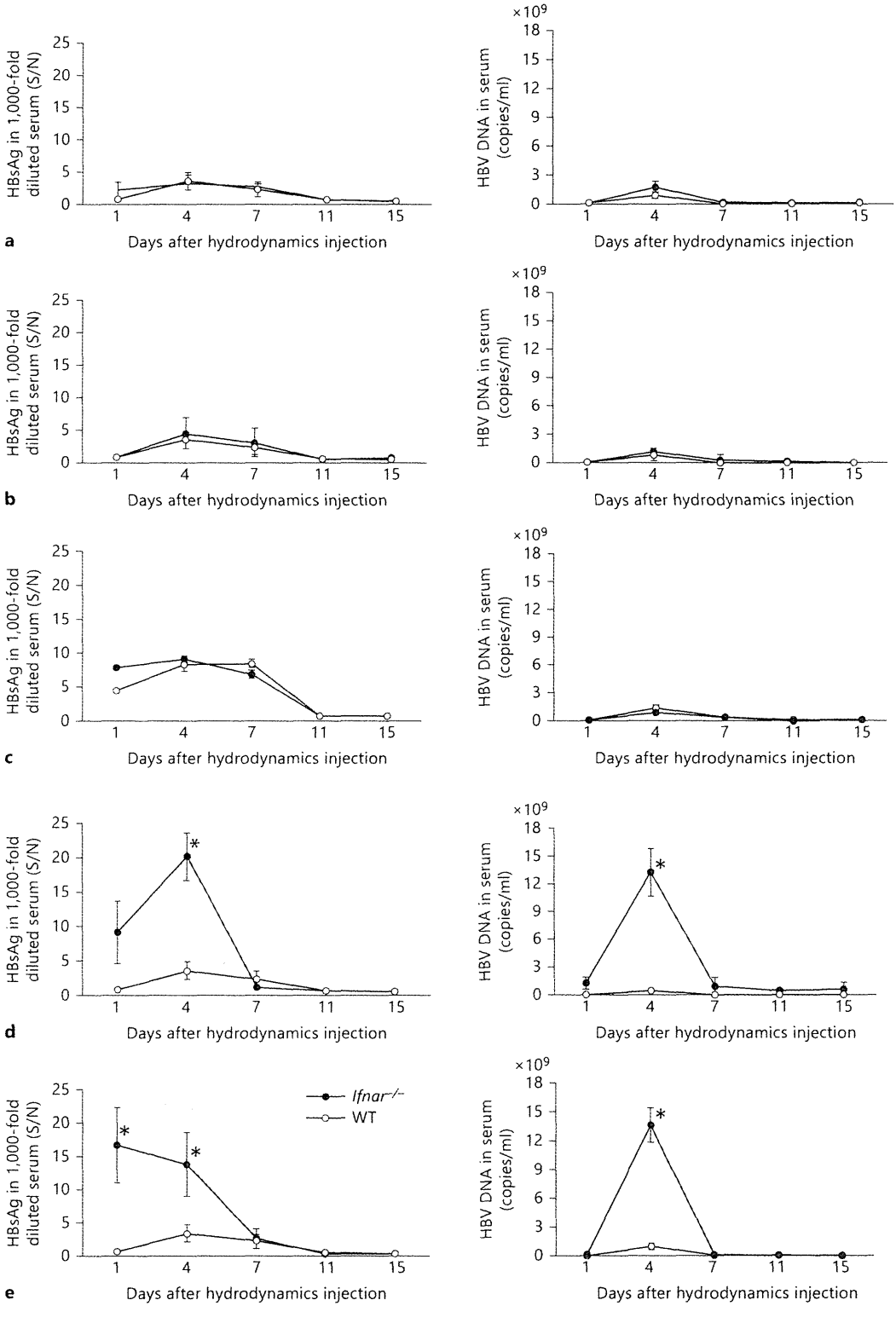

1

(For legend see next page.)

kinetics that closely paralleled the WT mice response (fig. 1a, b, left panels). Serum HBV-DNA levels were quantified using real-time PCR. The average titer of serum HBV DNA in 15 WT mice injected with HBV DNA was below 1×10^4 copies/ml 1 day after injection and reached 2×10^9 copies/ml 4 days after injection (fig. 1a–c, right panels). At later time points, most mice showed no detectable virus titer. Similar results were obtained with *Mavs*$^{-/-}$ and *Ticam-1*$^{-/-}$ mice (fig. 1a, b). The serum HBV-DNA and HBsAg results showed only a marginal effect for the absence of MAVS or TICAM-1 compared to WT mice. The results suggested that the pathways involving these two adaptor proteins were dispensable for triggering the immune responses that suppressed HBV replication.

To determine whether the RIG-I/MDA5-MAVS and TLR3-TICAM-1 RNA-sensing pathways were dispensable for suppressing the HBV replication, similar studies were performed in mice lacking both the MAVS and TICAM-1 adaptor proteins (fig. 1c). No notable differences were observed between WT and MAVS/TICAM-1 double-knockout mice in serum HBsAg and HBV-DNA levels, consistent with other data obtained. In addition, similar kinetics of intrahepatic clearance of the HBV template as well as HBV replication was observed in WT, *Mavs*$^{-/-}$, and *Ticam-1*$^{-/-}$ mice as revealed by Southern blotting using HBV-specific probes (online suppl. fig. 1).

To ensure the efficiency of delivery of the HBV transcriptional template into the mouse liver, a plasmid harboring the *lacZ* gene was used to transfect the liver cells using the hydrodynamic injection method. X-gal (a substrate for *lacZ*) staining showed that nearly the entire liver of injected mice has successfully received the injected plasmid (online suppl. fig. 2). An independent determination of transfection efficiency was carried out using a plasmid harboring the GFP fragment. The comparable transfection efficiencies observed did not differ significantly among the different mouse strains (data not shown). Furthermore, quantification of HBV mRNA in the organs of WT and knockout mice on day 3 after hydrodynamic injection revealed that HBV mRNA was amplified mainly in the liver but not in other organs, including kidney, lung, heart, spleen, and thymus (online suppl. fig. 3). Only weak HBV signals were detected in other organs in some types of knockout mice. These results demonstrated that HBV replication in vivo using the injection method was efficient and liver specific.

To further assess the possibility of HBV RNA acting as pathogen-associated molecular patterns to trigger the induction of type I IFN in hepatocytes, we transfected the immortalized hepatocytes with a plasmid containing the full genome of HBV as well as RNA containing the HBV mRNA. Along with the synthetic analog of dsRNA, poly(I:C), as a control, we determined the activity of the IFN-β promoter upon the stimulation using reporter gene assay (online suppl. fig. 4). Unlike poly(I:C), neither the full genome of HBV nor RNA induced any activity of the type I IFN promoter in the immortalized hepatocytes. Furthermore, we quantified the endogenous expression of genes including *cGas*, *Sting*, and *Mavs* in the hepatocyte cell lines in order to access the intrinsic RNA or DNA-sensing pathways (online suppl. fig. 5). We found that the hepatocyte cell lines, including those originating from mice and humans, expressed extremely low amounts of *Sting* compared to the intrinsic *Mavs*. However, other cell lines, including RAW 264.7 (murine macrophage cell line) and L929 (murine fibrosarcoma cell line), have higher endogenous expression of *Sting* in comparison to *Mavs*.

IRF-3/IRF-7 and IFNAR Are Critical Factors for HBV Replication Regulation

To investigate the mechanisms underlying the rapid termination of HBV replication in WT mice, we examined HBV clearance in IRF-3-/IRF-7-deficient mice. Activation of transcription factors including IRF-3 or IRF-7 is essential for raising immune responses including IFN production [25]. Unlike *Mavs*$^{-/-}$, *Ticam-1*$^{-/-}$, or WT mice, mice lacking the transcription factors IRF-3/IRF-7 had

Fig. 1. IFNAR and IRF-3/IRF-7 are critically associated with regulation of HBV propagation in mice but not MAVS and/or TICAM-1. HBsAg or HBV DNA were measured with sera from *Mavs*$^{-/-}$ (n = 13) (**a**), *Ticam-1*$^{-/-}$ (n = 10) (**b**), *Ticam-1*$^{-/-}$/*Mavs*$^{-/-}$ (n = 6) (**c**), *Irf-3*$^{-/-}$/*Irf-7*$^{-/-}$ (n = 12) (**d**), and *Ifnar*$^{-/-}$ (n = 13) (**e**) mice compared to WT mice (n = 15). These mice were hydrodynamically injected with 50 μg of the pTER-1.4xHBV plasmid containing full-genome HBV DNA. Mouse sera were isolated at the time points indicated. The HBsAg titers in the 1,000-fold diluted serum (left) and HBV DNA (right) in the knockout mice (●) were compared to the WT mice (○). Serum HBsAg titers were determined with an enzyme immunoassay at O.D. 450 nm [calculated as signal-over-noise ratios (S/N)]. Sera HBV DNA were determined by Q-PCR and indicated as copies per milliliter. Error bars indicate SD. The statistical p values were analyzed and no significant differences were observed in **a–c**. * $p < 0.01$ in **d** and **e** are time points statistically different between WT and transgenic mice.

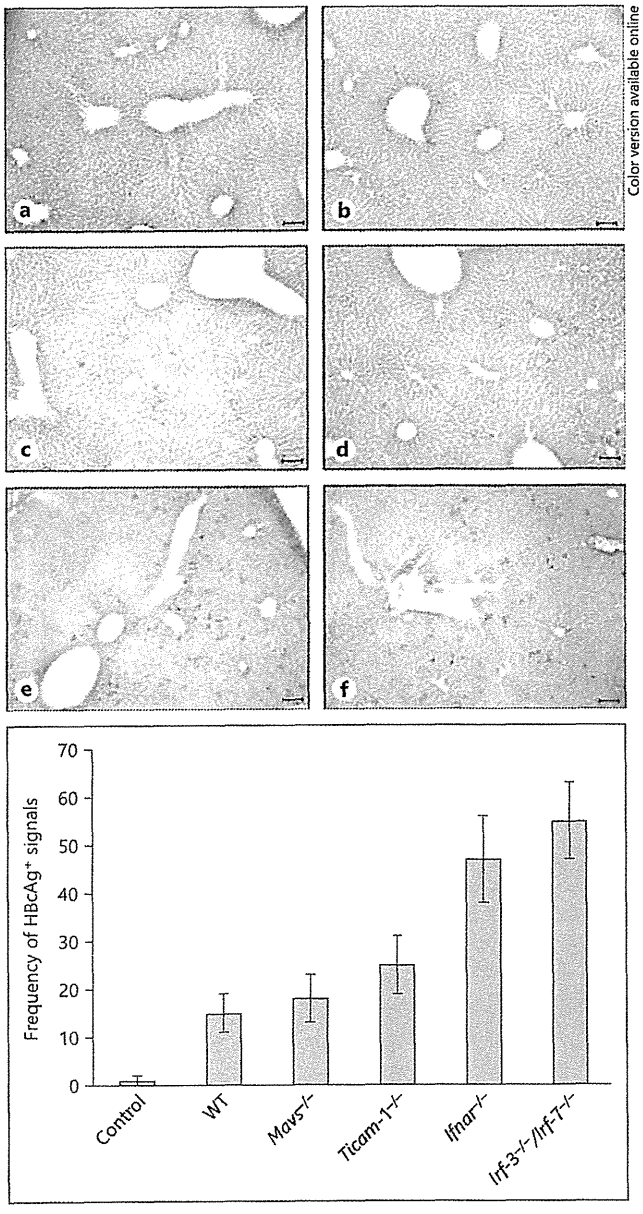

Fig. 2. Lacking IFNAR and IRF-3/IRF-7 causes an increase of HBcAg in mouse liver injected with the HBV replicative plasmid. The HBc protein in the livers on day 3 after injection was visualized with immunohistochemical staining of the mice liver sections embedded in OCT using an anti-HBc antibody for HBcAg. Representative sections are shown. HBcAg-positive cells were absent in the WT mice that received only the control plasmid (**a**). Only marginal differences were observed in the frequency of HBcAg-positive cells between WT (**b**), *Mavs*$^{-/-}$ (**c**), and *TICAM-1*$^{-/-}$ (**d**) mice. Frequency of HBcAg-positive cells in the livers of the *Ifnar*$^{-/-}$ (**e**) and *Irf-3*$^{-/-}$/*Irf-7*$^{-/-}$ (**f**) mice are more prevalent compared to the WT mice. The scale bars represent 10 μm. The images are displayed at 200× magnification. Frequency of HBcAg-positive signals between the different mouse strains shown is based on 3 images of each.

markedly high amounts of HBsAg and HBV DNA in sera (fig. 1d). A sharp peak of HBsAg in sera occurred in *Irf-3*$^{-/-}$/*Irf-7*$^{-/-}$ mice on day 4 after injection. However, in spite of the high virus titer at the early stage, HBsAg and DNA in sera were cleared with kinetics that paralleled the WT mice response, and viremia was eliminated by day 11. Hence, the substantial differences in the serum viremia between WT and *Irf-3*$^{-/-}$/*Irf-7*$^{-/-}$ mice in the early stage after transfection presumably reflects the importance of the genes being expressed with these transcription factors in the suppression of the HBV replication. IRF-3 and IRF-7 are the key molecules in the suppression of HBV viremia in the early stage after HBV injection.

Since type I IFN stimulates the IFNAR pathway to amplify type I IFN production, we hydrodynamically transfected HBV plasmid into mice lacking the gene of the type I IFN receptor (*Ifnar*$^{-/-}$) and assessed the suppression of HBV replication. *Ifnar*$^{-/-}$ mice showed markedly high titers of viral DNA and antigens in sera (fig. 1e) similar to *Irf-3*$^{-/-}$/*Irf-7*$^{-/-}$ mice.

The presence of HBcAg-positive hepatocytes was also monitored by immunohistochemical staining of liver sections from mice of each strain at day 4 after the injections (fig. 2). Data from the observed HBcAg-positive hepatocytes were in good agreement with the results on sera HBsAg and HBV DNA: only deficiency of IRF-3/IRF-7 and IFNAR resulted in a sharp increase of viremia in mice in the early stage (earlier than day 4). Fewer HBcAg-positive hepatocytes were observed in *Mavs*$^{-/-}$ and *Ticam1*$^{-/-}$ as well as WT mice at day 4 after injection than in *Irf-3*$^{-/-}$/*Irf-7*$^{-/-}$ or *Ifnar*$^{-/-}$ mice (fig. 2).

To gain insight into cytokine production in the liver in response to the HBV genome and its replication, we quantified the expression of type I IFN, IFN-γ, IL-7, IL-12p40, and chemokines including CXCL9, CXCL10, and CXCL11 mRNA in the livers of WT mice receiving either the control plasmid or plasmid carrying the HBV full genome on days 1, 3, 7, and 10 after hydrodynamic injection. Replication of HBV in the liver did not cause any significant changes in the expression of the cytokines or chemokines except the IFNs and CXCL-10 (fig. 3a–h). A similar study was carried out in WT and *Ifnar*$^{-/-}$ mice in order to further elaborate the type I IFN production. The IFNs increased in WT mice livers receiving the HBV full genome compared to the mouse livers receiving the control plasmid (fig. 3i–k). This increase was not observed in *Ifnar*$^{-/-}$ mice lacking the INF receptor. Although there appeared to be slight individual-to-individual differences in the apparent peaks of IFN-α induction, the result indicated that IFN-β was responsible for suppressing HBV

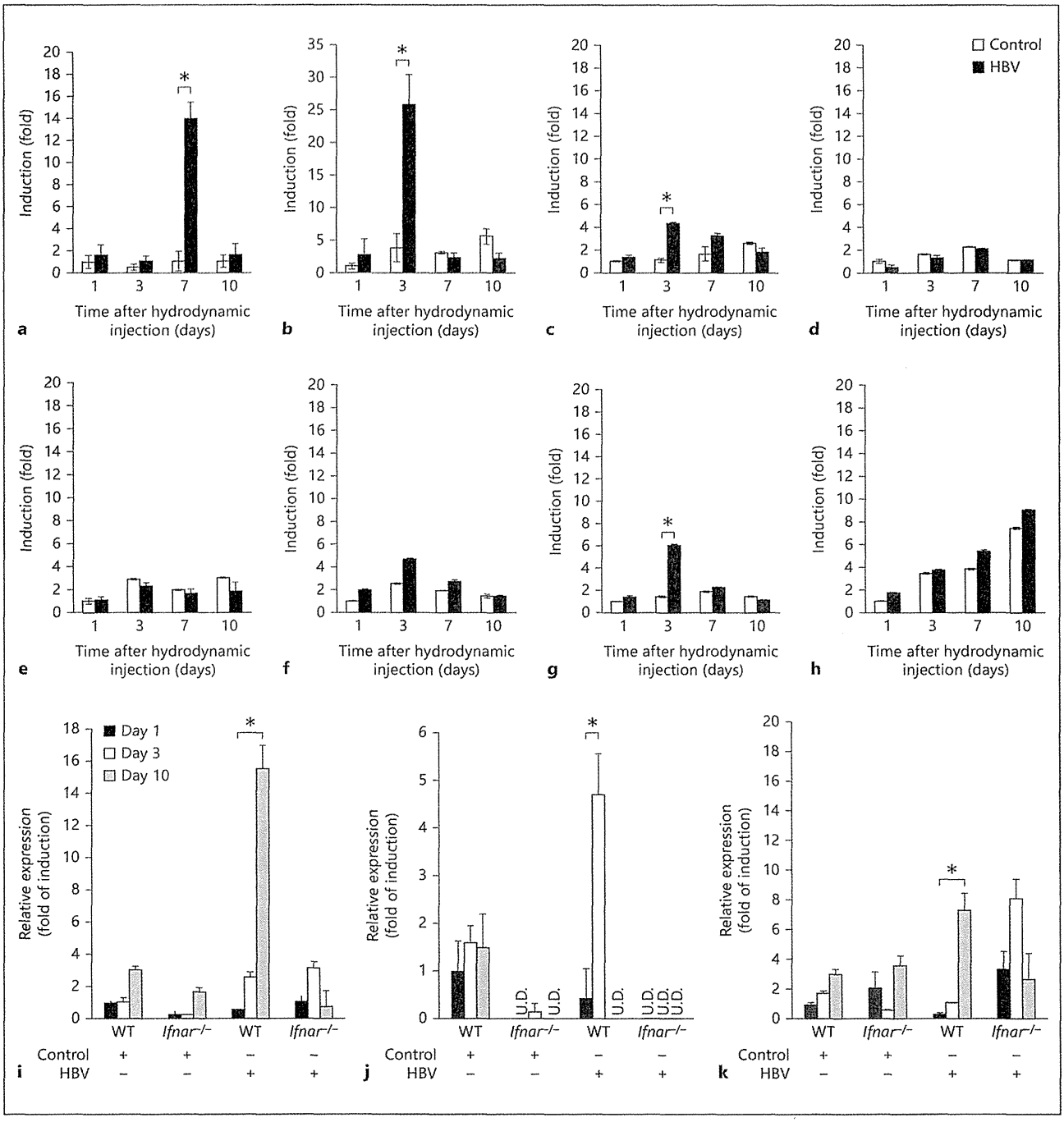

Fig. 3. Type I and II IFN expression is induced by HBV replication, and lacking the type I IFN receptor (IFNAR) causes failure of these inductions. WT mice were hydrodynamically injected with 50 μg of the pTER-1.4xHBV or control plasmid as described, and livers were isolated on days 1, 3, 7, and 10 after injection. The expression of IFN-α (**a**), IFN-β (**b**), IFN-γ (**c**), IL-7 (**d**), IL-12p40 (**e**), CXCL-9 (**f**), CXCL-10 (**g**), and CXCL-11 (**h**) mRNA was determined by reverse transcription followed by real-time PCR, and was expressed as the fold of induction relative to the WT mice receiving the control plasmid. Induction of IFNs and CXCL-10 was observed in the mice receiving the HBV plasmid. Similar studies were conducted in the WT and *Ifnar*$^{-/-}$ mice: IFN-α (**i**), IFN-β (**j**), and IFN-γ (**k**). *Ifnar*$^{-/-}$ mice show reduced expression of the IFNs compared to the WT. Data represent the mean of 3 mice on each strain and time point mentioned. * $p < 0.05$. U.D. = Undetected.

replication early. However, the reason for the lag in the induction of IFN-γ between the WT and *Ifnar*$^{-/-}$ mice remains unclear.

Taken together, these results suggest that type I IFN was indispensable for suppressing HBV replication in the early stage after viral genome entry. Type I IFN binds to its receptor to induce intracellular antiviral proteins to disrupt HBV replication. The results, however, infer that intrahepatic HBV clearance at the later stage is independent of IFN.

HBV Clearance in a Later Stage by Acquired Immunity

Previous studies by Yang et al. [23] and other groups showed that HBV replication persists indefinitely in globally immunodeficient mice such as NOD/Scid mice hydrodynamically injected with the replication-competent plasmid carrying the full genome of HBV. To investigate whether the elevated viral titer in *Ifnar*$^{-/-}$ and *Irf-3*$^{-/-}$/*Irf-7*$^{-/-}$ mice on day 4 after hydrodynamic injection and intrahepatic HBV clearance were related to immune effectors including T and B cells, HBV clearance was examined in *Rag-2*$^{-/-}$ mice. The lack of V(D)J recombination in this strain resulted in failure to produce mature B or T lymphocytes. As shown in figure 4, the absence of mature T and B cells in the *Rag-2*$^{-/-}$ mice did not result in elevated viral titer immediately after transfection, unlike in *Ifnar*$^{-/-}$ and *Irf-3*$^{-/-}$/*Irf-7*$^{-/-}$ mice. However, *Rag-2*$^{-/-}$ mice failed to clear the input plasmid and HBV products, as sera HBsAg and HBV DNA were detected up to day 15 (fig. 4a), by the time viral replication was terminated in all the other strains tested (fig. 4c, d). In other words, activation of the immune effectors such as the B and T cells is responsible for the intrahepatic HBV clearance, their activation being independent of IFN and IRF-3/IRF-7.

MyD88 Deficiency Leads to Slower HBV Clearance

The MyD88-dependent pathway has been known to lead to the production of inflammatory cytokines and is common to all TLRs, except TLR3 [22]. To examine whether a MyD88-dependent pathway is required in the intrahepatic clearance of the HBV, we monitored the serum HBsAg in MyD88-deficient mice. As shown in figure 4b, an increase in sera HBsAg in *Myd88*$^{-/-}$ mice was observed, although without particular antigenemia peaks at the early stage of transfection in *Ifnar*$^{-/-}$ and *Irf-3*$^{-/-}$/*Irf-7*$^{-/-}$ mice (fig. 4b, c). Instead, a delay in the elimination of the HBV was observed (fig. 4b, d). Typically, WT mice or other mouse strains lose serum HBsAg from day 11 after injection. However, serum antigen was detectable on day 15 in *Myd88*$^{-/-}$ mice. Delayed elimination of HBV plasmid and single-strand DNA in the liver was observed in Southern analysis of the liver from *Myd88*$^{-/-}$ mice compared with WT, *Mavs*$^{-/-}$, and *Ticam-1*$^{-/-}$ mice (online suppl. fig. 1).

Additionally, ELISA to determine anti-HBsAg antibody production in mouse sera after hydrodynamic injection revealed that anti-HBs antibody was produced in WT mice from day 7 and peaked at day 15 (fig. 4e). RAG2-deficient mice lacking mature T and B cells failed to produce any antibody, and *Myd88*$^{-/-}$ mice also had lower or nearly undetectable anti-HBs antibody in serum in comparison to the typical response of WT mice at later transfection stages. These results suggested that MyD88 and RAG2 were crucial for triggering acquired immunity against HBV in vivo.

Discussion

In the present study, several different knockout mice were analyzed in an attempt to define the mechanism of innate immunity against HBV in vivo. The evidence we obtained indicated that viral replication was not affected by MAVS or TICAM-1 knockout, but absence of IRF-3 or IRF-7 transcription factors, as well as the IFN receptor, had an adverse effect on the inhibition of HBV replication. The results herein demonstrated that the TICAM-1 and MAVS pathways were not required in either suppressing the virus replication or intrahepatic clearance of HBV replicative plasmid in vivo.

Although a DNA virus, HBV has the unique feature of replicating via an RNA proviral intermediate that is copied into DNA. Thus, defining the virus component, either HBV DNA or RNA that triggers the antiviral response is crucial to understand the immune mechanisms that are responsible for eliminating HBV during infection. HBV RNA has been suggested as the putative pathogen-associated molecular pattern of HBV in a few reports [16–18, 26]. HBx or HBs inhibits IFN-β induction followed by activation of TLR3 or RIG-I pathways with poly(I:C) or SeV, respectively. However, these findings must be interpreted with caution, as poly(I:C) and SeV are heterologous inducers for evaluating either the TLR3 or RIG-I pathway [16, 17]. No definitive conclusion on activation of the TLR3 or RIG-I pathway by HBV RNA in vivo has been reported yet.

Viral RNA is recognized largely by RIG-I or MDA5 in the cytosol of infected cells [27, 28] and by TLR3 or

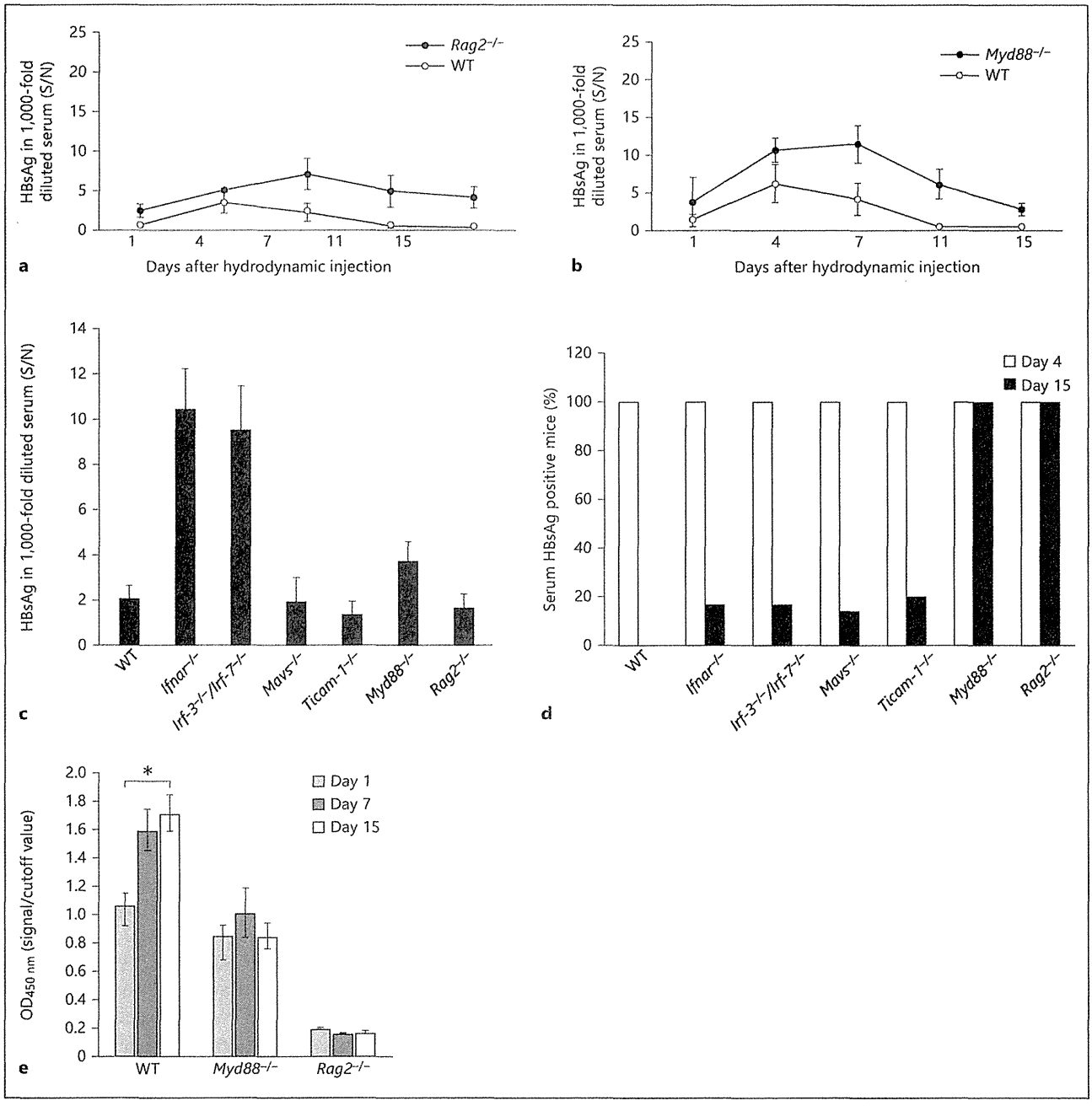

Fig. 4. Mice lacking RAG2 and MyD88 show insufficient clearance of HBV. **a**, **b** The *Rag2*$^{-/-}$, *Myd88*$^{-/-}$, and WT mice were hydrodynamically injected with 50 μg of pTER-1.4xHBV and HBsAg in the mouse sera at the time points indicated and analyzed with ELISA as described. **c** HBsAg in 1,000-fold diluted serum from all the mice strains including WT, *Ifnar*$^{-/-}$, *Irf-3*$^{-/-}$/*Irf-7*$^{-/-}$, *Mavs*$^{-/-}$, *Ticam-1*$^{-/-}$, *Myd88*$^{-/-}$, and *Rag2*$^{-/-}$ at day 4 after the hydrodynamic injections. Only *Ifnar*$^{-/-}$ and *Irf-3*$^{-/-}$/*Irf-7*$^{-/-}$ mice show a remarkable increase, while a moderate increase of sera HBsAg was seen in *Myd88*$^{-/-}$ mice. **d** HBsAg persistence rates in all the mice strains receiving pTER1.4HBV were determined by the percentage of serum HBsAg-positive mice on day 4 (□) and day 15 (■) after the hydrodynamic injections. Serum HBsAg was found to be persistent only in mice deficient in MyD88 and RAG2 on day 15 as 100% of the mice from these two strains were HBsAg positive (n = 8 for each mice strain). **e** Lacking MyD88 and RAG2 leads to the failure of the knockout mice to produce anti-HBs IgG compared to the WT mice on day 15 after injection as determined by ELISA using antigen of HBs (n = 3 for each mice strain). * $p < 0.05$. S/N = Signal-over-noise ratio.

TLR7/8 in the endosome of other noninfected cells [29, 30]. These RNA sensors require MAVS, TICAM-1, or MyD88 as adaptor proteins to induce type I IFN [28]. On the other hand, cytoplasmic DNA is recognized by DNA sensors including DAI, IFI16, RIG-I, DHX9 (helicase), and cGAS [31]. STING is the only adaptor for all IFN-inducing DNA sensors in mouse cells reported so far [30, 32, 33], although some of these sensors are reported to induce type I IFN via MAVS in human cells. These adaptors, TICAM-1, MAVS, and STING, are all linked to activation of IRF-3/IRF-7 which act as transcription factors that induce activation of the type I IFN promoter during viral infections. Involvement of different pathways in the induction of type I IFN is critically dependent on the virus species and cell type. Cell type-specific contributions of other sensors, including DEAD box helicases, might occur in some cases of infection. However, in hepatocytes, the control plasmid per se exhibited no IFN-inducing response, suggesting that the HBV replication is a critical step for IFN induction. Actually, no contribution of other sensors except RIG-I/MDA5 and TLR3 has been reported so far.

Using the murine hydrodynamic injection model, we found that mice deficient in IRF-3 and IRF-7 or IFNAR do not inhibit HBV replication as effectively as their WT counterparts and result in elevated HBV titers in mice sera and livers. These findings imply that type I IFN acting on IFNAR is indispensable for evoking anti-HBV protective responses although such a hypothesis is in disagreement with previous findings that HBV does not induce detectable changes in type I IFN expression during the early weeks of infection [34]. There are a few possibilities of how type I IFN is produced in mice receiving HBV template plasmid. One of them is that HBV could be recognized by pathways that do not link to MAVS or TICAM-1 and facilitate IFN production in the cytoplasm. For instance, STING-dependent signaling leads to type I IFN induction, and it has been shown that this can be MAVS and TICAM-1 independent. Notably, STING-dependent signaling is especially associated with DNA-mediated induction of type I IFN via IRF-3/IRF-7, and genomic DNA is an important part of HBV replication. It would be interesting to clarify such hypotheses using *Sting*$^{-/-}$ mice in the near future.

To elucidate the molecular pattern which triggers type I IFN induction, we transfected either HBV DNA or RNA into immortalized hepatocytes. To our surprise, we were unable to detect significant IFN-β induction with either HBV replicative DNA or HBV RNA. As we looked into the possible reasons to account for the lack of innate immune responses against HBV in hepatocytes, we found that the endogenous expression of STING in hepatocyte cell lines including HepG2 and immortalized mouse hepatocytes is extremely low compared to other cell lines like macrophages or dendritic cells, thus suggesting that STING-dependent signaling might play a crucial role in inducing type I IFN in response to HBV. The produced IFN in turn activates the IFNAR pathway. There are various cells populations in the liver that express IFNAR and therefore subsequently initiate a natural signaling cascade for amplification of IFN production via the Jak-STAT pathway.

Another possible way for HBV to induce IFN is via the HBV-stimulated nonparenchymal or resident myeloid cells. Even though there has been no report suggesting that HBV substantially infects pDCs, Isogawa et al. [5], demonstrated that freshly isolated CD11c^{+} cells of intrahepatic myeloid cells rather than the hepatocytes expressed TLRs including TLR2, 3, and 9. Therefore, resident myeloid cells might induce IFN to further prevent the spread of HBV by activating the IFNAR pathway in bystander cells or hepatocytes.

Although *Myd88*$^{-/-}$ mice receiving an HBV-DNA injection did not exhibit significantly high virus titers in the early phase unlike those observed in *Ifnar*$^{-/-}$ and *Irf-3*$^{-/-}$/*Irf-7*$^{-/-}$ mice, interestingly MyD88 is required for the intrahepatic clearance of the HBV replicative template. The fact that the transcriptional template persists in the absence of MyD88 suggests that MyD88 may play a pivotal role in intrahepatic HBV clearance in the mouse model. Notably, MyD88 is the adaptor molecule for TLR7 and 9 in pDCs [35, 36]. Deficiency of MyD88 in pDCs may result in failure to induce acquired immunity for HBV. Our findings show that HBV-specific antibodies are efficiently produced in WT, but not in *Myd88*$^{-/-}$ mice. In addition, the number of pDCs has been previously reported to be reduced in vivo during several systemic viral infections including HBV [37]. In one of the most recent reports, Lv et al. [38], showed that HBV-derived CpG induces potent IFN-α production by human pDCs, which may partially explain how pDCs interact with HBV in infection. However, the cause of weak participation in the early response of IFN induction in *Myd88*$^{-/-}$ mice remains to be determined.

Recombinant IFN-α is a standard treatment for chronic HBV patients. Nevertheless, direct treatment with IFN yields only about 30% improvement in HBV patients and little is known about why most chronic HBV patients do not respond to IFN therapy [39]. As demonstrated in our study, virus persistency can be independent of the type I

IFN-inducing system. This observation leads to the suggestion that type I IFN is indispensable for inducing antiviral molecules to control viral replication and spread before the onset of more specific and powerful adaptive immune responses. This appeared to be factual at least in our knockout mouse models as virus titers were highly elevated in *Ifnar*$^{-/-}$ mice in the initial days after injection. Conversely, type I IFN did not have any influential effects on clearance of the HBV template in the later stages. Such observations coincide with the latest study conducted in patients with chronic HBV infection by Tan et al. [40], in which IFN-α treatment was shown to modulate innate immune parameters in the patients, but without any detectable effect on HBV-specific adaptive immunity. The missing link between the induction of type I IFN and anti-HBV cellular effectors needs to be further investigated in mouse models, including the mechanism of MyD88 participation in activation of the cellular immune response during infection. Elucidating molecular mechanisms between innate pattern sensing and evoking cellular effectors may provide a reasonable explanation for the failure of IFN-treatment in HBV infection.

Collectively, our study validates the use of the hydrodynamic transfection method in mimicking acute HBV infection in mouse models and demonstrated the host-virus relationship during HBV infection in many aspects. Since HBV infectious models with immunologically well-defined laboratory animals do not exist, the result presented in this study herein provides an insight into the dispensability of RNA sensors for induction of IFN by HBV RNA and the complexity of innate and adaptive immunity during HBV clearance.

Acknowledgements

This work was supported in part by Grants-in-Aid from the Ministry of Education, Science, and Culture and the Ministry of Health, Labor, and Welfare of Japan, and the Yasuda Cancer Foundation (T.S.) and the Ono Foundation (T.S.). Financial support by a MEXT Grant-in-Project 'The Carcinogenic Spiral', 'The National Cancer Center Research and Development Fund (23-A-44)', and the Japan Initiative for Global Research Network on Infectious Diseases (J-GRID) are gratefully acknowledged. We are grateful to Drs. H. Shime, J. Kasamatsu, K. Funami, and M. Tatematsu in our laboratory for their fruitful discussions. We thank Dr. F.V. Chisari (Scripps Research Institute, La Jolla, Calif., USA) for providing us with HBV plasmid and sleeping beauty.

Disclosure Statement

The authors declare no financial or commercial conflict of interest.

References

▶1 Guidotti LG, Chisari FV: Immunobiology and pathogenesis of viral hepatitis. Annu Rev Pathol 2006;1:23–61.

▶2 Zuckerman JN, Zuckerman AJ: Current topics in hepatitis B. J Infect 2000;41:130–136.

▶3 Ganem D, Prince AM: Hepatitis B virus infection – natural history and clinical consequences. N Engl J Med 2004;350:1118–1129.

▶4 Seeger C, Mason WS: Hepatitis B virus biology. Microbiol Mol Biol Rev 2000;64:51–68.

▶5 Isogawa M, Robek MD, Furuichi Y, Chisari FV: Toll-like receptor signaling inhibits hepatitis B virus replication in vivo. J Virol 2005;79:7269–7272.

▶6 Wu J, Lu M, Meng Z, Trippler M, Broering R, Szczeponek A, Krux F, Dittmer U, Roggendorf M, Gerken G, Schlaak JF: Toll-like receptor-mediated control of HBV replication by nonparenchymal liver cells in mice. Hepatology 2007;46:1769–1778.

▶7 Kawai T, Takahashi K, Sato S, Coban C, Kumar H, Kato H, Ishii KJ, Takeuchi O, Akira S: IPS-1, an adaptor triggering RIG-I- and Mda5-mediated type I interferon induction. Nat Immunol 2005;6:981–988.

▶8 Akira S, Uematsu S, Takeuchi O: Pathogen recognition and innate immunity. Cell 2006;124:783–801.

▶9 Takeuchi O, Akira S: Innate immunity to virus infection. Immunol Rev 2009;227:75–86.

▶10 Oshiumi H, Matsumoto M, Funami K, Akazawa T, Seya T: TICAM-1, an adaptor molecule that participates in Toll-like receptor 3-mediated interferon-β induction. Nat Immunol 2003;4:161–167.

▶11 Ishikawa H, Ma Z, Barber GN: STING regulates intracellular DNA-mediated, type I interferon-dependent innate immunity. Nature 2009;461:788–792.

▶12 Cheng G: Double-stranded DNA and double-stranded RNA induce a common antiviral signaling pathway in human cells. Proc Natl Acad Sci USA 2007;104:9035–9040.

▶13 Ablasser A, Bauernfeind F, Hartmann G, Latz E, Fitzgerald KA, Hornung V: RIG-I-dependent sensing of poly(dA:dT) through the induction of an RNA polymerase III-transcribed RNA intermediate. Nat Immunol 2009;10:1065–1072.

▶14 Chiu YH, Macmillan JB, Chen ZJ: RNA polymerase III detects cytosolic DNA and induces type I interferons through the RIG-I pathway. Cell 2009;138:576–591.

▶15 Stetson DB, Medzhitov R: Type I interferons in host defense. Immunity 2006;25:373–381.

▶16 Kumar M, Jung SY, Hodgson AJ, Madden CR, Qin J, Slagle BL: Hepatitis B virus regulatory HBx protein binds to adaptor protein IPS-1 and inhibits the activation of beta interferon. J Virol 2011;85:987–995.

▶17 Wei C, Ni C, Song T, Liu Y, Yang X, Zheng Z, Jia Y, Yuan Y, Guan K, Xu Y, Cheng X, Zhang Y, Wang Y, Wen C, Wu Q, Shi W, Zhong H: The hepatitis B virus X protein disrupts innate immunity by down regulating mitochondrial antiviral signaling protein. J Immunol 2010;185:1158–1168.

▶18 Yu S, Chen J, Wu M, Chen H, Kato N, Yuan Z: Hepatitis B virus polymerase inhibits RIG-I- and Toll-like receptor 3-mediated beta interferon induction in human hepatocytes through interference with interferon regulatory factor 3 activation and dampening of the interaction between TBK1/IKKepsilon and DDX3. J Gen Virol 2010;91:2080–2090.

▶19 Oshiumi H, Okamoto M, Fujii K, Kawanishi T, Matsumoto M, Koike S, Seya T: The TLR3/TICAM-1 pathway is mandatory for innate immune responses to poliovirus infection. J Immunol 2011;187:5320–5327.

20 Akazawa T, Ebihara T, Okuno M, Okuda Y, Shingai M, Tsujimura K, Takahashi T, Ikawa M, Okabe M, Inoue N, et al: Antitumor NK activation induced by the Toll-like receptor 3-TICAM-1 (TRIF) pathway in myeloid dendritic cells. Proc Natl Acad Sci USA 2007;104:252–257.

21 Noguchi C, Ishino H, Tsuge M, Fujimoto Y, Imamura M, Takahashi S, Chayama K: G to A hypermutation of hepatitis B virus. Hepatology 2005;41:626–633.

22 Tian Y, Chen WL, Kuo CF, Ou JH: Viral-load-dependent effects of liver injury and regeneration on hepatitis B virus replication in mice. J Virol 2012;86:9599–9605.

23 Yang PL, Althage A, Chung J, Chisari FV: Hydrodynamic injection of viral DNA: a mouse model of acute hepatitis B virus infection. Proc Natl Acad Sci USA 2002;99:13825–13830.

24 Aly HH, Oshiumi H, Shime H, Matsumoto M, Wakita T, Shimotohno K, Seya T: Development of mouse hepatocyte lines permissive for hepatitis C virus (HCV). PLoS One 2011;6:e21284.

25 Honda K, Taniguchi T: IRFs: master regulators of signalling by Toll-like receptors and cytosolic pattern-recognition receptors. Nat Rev Immunol 2006;6:644–658.

26 Wang X, Li Y, Mao A, Li C, Tien P: Hepatitis B virus X protein suppresses virus-triggered IRF3 activation and IFN-beta induction by disrupting the VISA-associated complex. Cell Mol Immunol 2010;7:341–348.

27 Kawai T, Akira S: Innate immune recognition of viral infection. Nat Immunol 2006;7:131–137.

28 Onomoto K, Yoneyama M, Fujita T: Regulation of antiviral innate immune responses by RIG-I family of RNA helicases. Curr Top Microbiol Immunol 2007;316:193–205.

29 Matsumoto M, Oshiumi H, Seya T: Antiviral responses induced by the TLR3 pathway. Rev Med Virol 2011, DOI: 10.1002/rmv.680.

30 Diebold SS: Recognition of viral single-stranded RNA by Toll-like receptors. Adv Drug Deliv Rev 2008;60:813–823.

31 Paludan SR, Bowie AG: Immune sensing of DNA. Immunity 2013;38:870–880.

32 Ishikawa H, Barber GN: The STING pathway and regulation of innate immune signaling in response to DNA pathogens. Cell Mol Life Sci 2011;68:1157–1165.

33 Suzuki T, Oshiumi H, Miyashita M, Aly HH, Matsumoto M, Seya T: Cell type-specific subcellular localization of phospho-TBK1 in response to cytoplasmic viral DNA. PLoS One 2013;8:e83639.

34 Bertoletti A, Gehring AJ: The immune response during hepatitis B virus infection. J Gen Virol 2006;87:1439–1449.

35 Hoshino K, Sasaki I, Sugiyama T, Yano T, Yamazaki C, Yasui T, Kikutani H, Kaisho T: Critical role of IkappaB Kinase alpha in TLR7/9-induced type I IFN production by conventional dendritic cells. J Immunol 2010;184:3341–3345.

36 Hoshino K, Sugiyama T, Matsumoto M, Tanaka T, Saito M, Hemmi H, Ohara O, Akira S, Kaisho T: IkappaB kinase-alpha is critical for interferon-alpha production induced by Toll-like receptors 7 and 9. Nature 2006;440:949–953.

37 Swiecki M, Wang Y, Vermi W, Gilfillan S, Schreiber RD, Colonna M: Type I interferon negatively controls plasmacytoid dendritic cell numbers in vivo. J Exp Med 2011;208:2367–2374.

38 Lv S, Wang J, Dou S, Yang X, Ni X, Sun R, Tian Z, Wei H: Nanoparticles encapsulating HBV-CpG induce therapeutic immunity against hepatitis B virus infection. Hepatology 2014;59:385–394.

39 Ter Borg MJ, Hansen BE, Bigot G, Haagmans BL, Janssen HL: ALT and viral load decline during PEG-IFN alpha-2b treatment for HBeAg-positive chronic hepatitis B. J Clin Virol 2008;42:160–164.

40 Tan AT, Hoang LT, Chin D, Rasmussen E, Lopatin U, Hart S, Bitter H, Chu T, Gruenbaum L, Ravindran P, Zhong H, Gane E, Lim SG, Chow WC, Chen PJ, Petric R, Bertoletti A, Hibberd ML: Reduction of HBV replication prolongs the early immunological response to IFNα therapy. J Hepatol 2014;60:54–61.

Immunobiology 220 (2015) 74–82

Contents lists available at ScienceDirect

Immunobiology

journal homepage: www.elsevier.com/locate/imbio

PolyI:C and mouse survivin artificially embedding human 2B peptide induce a CD4+ T cell response to autologous survivin in HLA-A*2402 transgenic mice

Jun Kasamatsu[a,1], Shojiro Takahashi[a,b,1], Masahiro Azuma[a,1,2], Misako Matsumoto[a], Akiko Morii-Sakai[a], Masahiro Imamura[b], Takanori Teshima[b], Akari Takahashi[c], Yoshihiko Hirohashi[c], Toshihiko Torigoe[c], Noriyuki Sato[c], Tsukasa Seya[a,*]

[a] Department of Microbiology and Immunology, Hokkaido University Graduate School of Medicine, Kita-ku, Sapporo, Japan
[b] Department of Hematology, Hokkaido University Graduate School of Medicine, Kita-ku, Sapporo, Japan
[c] Department of Pathology, Sapporo Medical University School of Medicine, Chuoh-ku, Sapporo, Japan

ARTICLE INFO

Article history:
Received 28 March 2014
Received in revised form 4 August 2014
Accepted 6 August 2014
Available online 23 August 2014

Keywords:
Survivin
PolyI:C
CD4 epitope
Peptide vaccine
Th1 response
Interferon-γ
Tumor immunity

ABSTRACT

$CD4^+$ T cell effectors are crucial for establishing antitumor immunity. Dendritic cell maturation by immune adjuvants appears to facilitate subset-specific $CD4^+$ T cell proliferation, but the adjuvant effect for CD4 T on induction of cytotoxic T lymphocytes (CTLs) is largely unknown. Self-antigenic determinants with low avidity are usually CD4 epitopes in mutated proteins with tumor-associated class I-antigens (TAAs). In this study, we made a chimeric version of survivin, a target of human CTLs. The chimeric survivin, where human survivin-2B containing a TAA was embedded in the mouse survivin frame (MmSVN2B), was used to immunize HLA-A-2402/K^b-transgenic (HLA24^b-Tg) mice. Subcutaneous administration of MmSVN2B or xenogeneic human survivin (control HsSNV2B) to HLA24^b-Tg mice failed to induce an immune response without co-administration of an RNA adjuvant polyI:C, which was required for effector induction *in vivo*. Although HLA-A-2402/K^b presented the survivin-2B peptide in C57BL/6 mice, 2B-specific tetramer assays showed that no $CD8^+$ T CTLs specific to survivin-2B proliferated above the detection limit in immunized mice, even with polyI:C treatment. However, the $CD4^+$ T cell response, as monitored by IFN-γ, was significantly increased in mice given polyI:C + MmSVN2B. The Th1 response and antibody production were enhanced in the mice with polyI:C. The CD4 epitope responsible for effector function was not $Hs/MmSNV_{13\text{-}27}$, a nonconserved region between human and mouse survivin, but region 53-67, which was identical between human and mouse survivin. These results suggest that activated, self-reactive $CD4^+$ helper T cells proliferate in MmSVN2B + polyI:C immunization and contribute to Th1 polarization followed by antibody production, but hardly participate in CTL induction.

Introduction

Dendritic cells (DCs) present exogenous antigens (Ags) to cells in the major histocompatibility complex (MHC) class I-restricted Ag-presentation pathway and cause the proliferation of $CD8^+$ T cells specific to the extrinsic Ag. When tumor cells have soluble and insoluble exogenous Ags, MHC class I Ag presentation is mainly transporter associated with antigen processing (TAP)- and proteasome-dependent, suggesting the pathway is partly shared with the pathway for endogenous Ag presentation. The delivery of exogenous Ag by DCs to the pathway for MHC class I-restricted Ag presentation is called cross-presentation (Bevan 1976).

PolyI:C is a double-stranded RNA analog that activates RNA-sensing pattern-recognition receptor pathways (Matsumoto and Seya 2008; Seya and Matsumoto 2009). PolyI:C is an efficient trigger of cross-presentation, and facilitates cross-priming of $CD8^+$ T cells in the presence of Ag. Tumor-associated antigens (TAAs) usually expressed in low levels are thought to need support from pattern-recognition receptor activation to induce TAA-specific cytotoxic T lymphocytes (CTLs) (Seya et al. 2013).

* Corresponding author at: Department of Microbiology and Immunology, Hokkaido University Graduate School of Medicine, Kita 15, Nishi 7, Kita-ku, Sapporo 060-8638, Japan. Tel.: +81 11 706 7866; fax: +81 11 706 7866.
E-mail address: seya-tu@pop.med.hokudai.ac.jp (T. Seya).
[1] These authors equally contributed.
[2] Present address: University of Montreal, 2900 Edouard-Montpetit, Faculty of Medicine/Pavilion Roger Gaudry, Department of Pathology and Cellular Biology, Montreal, QC, H3T 1J4, Canada.

http://dx.doi.org/10.1016/j.imbio.2014.08.017
0171-2985/

Many TAAs have been identified and tested for tolerability to patients and for ability to suppress tumor progression. Peptide vaccine immunotherapy against cancer has been studied clinically (Rosenberg et al. 2004). Survivin (SVN) is a TAA that generates CTLs in cancer patients (Schmitz et al. 2000; Andersen et al. 2001). Human survivin (HsSVN) is a 16.5 kDa cytoplasmic protein that inhibits caspase 3 and 7 in cells stimulated to undergo apoptosis (Altieri 2001). SVN is a member of the inhibitor of apoptosis protein family associated with fetal development. Therefore, except for testis, thymus and placenta, normal tissues express little SVN (Ambrosini et al. 1997; Altieri 2001). SVN is required in early thymocyte development from CD4/CD8-double-negative cells to CD4/CD8-double-positive lymphocytes (Okada et al. 2004). SVN is expressed in a wide variety of malignant cells (Altieri 2001; Fukuda and Pelus 2006). There are several splicing variants including a variant HsSVN2B with a cryptic epitope for MHC class I in humans. An HsSVN2B peptide (AYACNTSTL: 80–88) is an HLA-A*2402-restricted peptide recognized by CD8+ CTLs (Hirohashi et al. 2002). Some cancer cells have higher mRNA levels of the HsSVN splice variant 2B, but whether this splice variant functions in tumorigenesis is unknown (Li 2005).

Several trials have studied the SVN2B peptide in cancer patients (Tsuruma et al. 2008; Honma et al. 2009; Kameshima et al. 2013). Although CTLs specific for SVN were detected in peripheral blood mononuclear cells of most cancer patients, as determined by HLA-A*2402/SVN2B tetramer assays, no substantial therapeutic effect on cancer is seen in most clinical studies. A phase I clinical study found that vaccination with SVN2B peptide combined with IFN-α had significant therapeutic benefits in advanced pancreatic cancer patients, in spite of IFN-mediated side effects. Thus, an IFN-inducing adjuvant, that simultaneously up-regulates Ag-presentation and IFN-inducible genes, might more efficiently contribute to the clinical benefits of SVN for cancer patients.

PolyI:C is an analog of virus double-stranded RNA with IFN-inducing adjuvant properties. To test the effect of polyI:C on survivin-derived CTLs, we used a mouse model expressing human HLA-A24 that presents the SVN2B peptide (Gotoh et al. 2002). Mice have no splice counterpart for HsSVN2B and therefore mouse survivin (MmSVN) lacks the 2B portion of HsSVN, although the mouse ortholog is 84% homologous to HsSVN (Kobayashi et al. 1999). When BALB/c mice are injected intraperitoneally with HsSVN2B + RNA adjuvant, high levels of $CD4^+$ T cells are induced in splenic T cells, as determined by IFN-γ, TNF-α, and IL-2 production, as well as development of lytic MHC class II-restricted T cells and memory (Charalambous et al. 2006).

The N-terminal sequence of HsSVN, which includes amino acids 13–27 (FLKDHRISTFKNWPF), differs from that of MmSVN (YLKNYRIATFKNWPF) (Charalambous et al. 2006). Therefore, high frequencies of self-reactive $CD4^+$ T cells specific for a tumorigenic protein might be elicited in mice with xenogeneic HsSVN. However, self-reactive $CD4^+$ T cells can be induced toward syngeneic or nonmutated CD4 epitopes in cancer patients (Topalian et al. 1996; Osen et al. 2010). To test the possibility that sub-derived self-CD4 epitopes participate in $CD8^+$ CTL proliferation, we made a chimeric survivin protein (MmSVN2B), where the human 2B exon sequence was embedded into MmSVN. We immunized HLA-A-2402/K^b-transgenic (HLA24^b-Tg) B6 mice with MmSVN2B. The results indicated that the $CD8^+$ CTL response to a self-tumor Ag (2B peptide) was barely enhanced by treatment of HLA24^b-Tg mice with MmSVN2B in the presence of polyI:C. However, $CD4^+$ T cell immune responses to the CD4 epitope of MmSVN2B and HsSVN2B were significantly enhanced in HLA24^b-Tg mice with SVN2B proteins + polyI:C. The CD4 epitopes were not the N-terminal $HsSVN_{13-27}$ and $MmSVN_{13-27}$ sequences, but the $Hs/MmSVN_{53-67}$ (DLAQCFFCFKELEGW) sequence, which is identical in HsSVN2B and MmSVN2B and thus a nonmutated CD4 epitope. PolyI:C was required for proliferation of self-reactive $CD4^+$ Th1 cells that recognized the syngeneic epitope. We discuss how RNA adjuvant might induce $CD4^+$ Th1 cells and act in the antitumor immune response.

Materials and methods

Bioinformatics analysis

Ensembl databases (http://asia.ensembl.org/index.html) were used to investigate human and mouse SVN genomic structure. Primate and rodent short interspersed nuclear elements (SINEs) were predicted using the Repeat Masker program (http://www.repeatmasker.org/). Results from databases were confirmed by comparison to previous reports (Mahotka et al. 1999).

Expression analysis

Total RNA was extracted from tissues from C57BL/6 mice and murine cell lines using RNeasy Mini Kits (Qiagen) following the manufacturer's instructions. RT-PCR used High Capacity cDNA Reverse Transcription Kits (Applied Biosystems) according to the manufacturer's instructions. Primer pairs were designed to span separate exons to avoid amplifying other genomic DNA. Primers were 5′-ACTACCGCATCGCCACCT-3′ (forward) and 5′-GCTTGTTGTTGGTCTCCTTTG-3′ (reverse) for detection of the murine SVN gene (MmSVN) and 5′-TGTAACCAACTGGGACGATAT-3′ (forward) and 5′-CTTTTCACGGTTGGCCTTAG-3′ (reverse) for murine *Gapdh*. PCR conditions for mSVN were 94 °C 3 min; 35 cycles of 94 °C 30 s, 65 °C 30 s, 72 °C for 30 s; and 7 min 72 °C. *Gapdh* PCR conditions were 94 °C 3 min; 30 cycles of 94 °C 30 s, 65 °C 30 s, and 72 °C 30 s; and 7 min at 72 °C.

Antigens

The HsSVN2B-coding sequence was amplified using primers 5′-CGGGATCCATGGGTGCCCCGACG-3′ (underline: *Bam*HI site) and 5′-GGAATTCTCAATCCATGGCAGC-3′(underline: *Eco*RI site). To construct the mSVN 2B gene (MmSVN2B), we used two-step PCR to make a chimeric gene of the mSVN gene and the human 2B exon (Fig. 2). In the first PCR, two fragments containing exon 1–2 and exon 3–4 were amplified using primers 5′-CCGCTCGAGATGGGAGCTCCGGCGCT-3′ (underline: *Xho*I site) and 5′-*ACCGTGCCCGGCCCA*ATCGGGTTGTCA-3′ (italics: 5′-end of exon 2B of the HsSVN2B gene) for exon 1 and exon 2 and 5′-*GGGCGGATCACGAG*AGAGGAGCATAGAAAGCA-3′ (italics: 3′-end of exon 2B) and 5′-CGGGATCCTTAGGCAGCCAGCTGCTCAAT-3′ (underline: *Bam*HI site) for exon 3 and exon 4. The exon 2B fragment was amplified using primers 5′-*CGATGACAACCCGATT*GGGCCGGGCACGG-3′ (italics: 3′-end of exon 1 and exon 2 of MmSVN) and 5′-*TTTCTATGCTCCTCT*CTCGTGATCCGCCC-3′ (italics: 5′-end of exon 3 and exon 4 of MmSVN). In the second PCR, the three templates from the first PCR were mixed in equal amounts and amplified using primers 5′-CCGCTCGAGATGGGAGCTCCGGCGCT-3′ (underline: *Xho*I site) and 5′-CGGGATCCTTAGGCAGCCAGCTGCTCAAT-3′ (underline: *Bam*HI site). The pCold vector II (TaKaRa) and SVN fragments were restriction digested and ligated overnight with T4 ligase (Promega) at 4 °C. Ligation mixtures were transformed into competent *Escherichia coli* strain BL21 (DE3) cells. After preculturing for 2 h at 37 °C, cells were cooled on ice. Recombinant protein expression was induced with isopropyl-1-thio-β-D-galactopyranoside at a final concentration of 1 mM and cultured for 24 h at 16 °C. N-His-tagged survivin proteins were purified using a Profinia protein purification system (Biorad). Buffer of

purified SVN proteins was sequentially exchanged with PBS containing 2 M urea. To rule out lipopolysaccharide contamination, we treated survivin proteins with 200 μg/ml of polymixin B (Sigma) for 30 min at 37 °C before use. OVA (ovalbumin) (Sigma) was similarly treated with polymixin B as an Ag.

Mice

C57BL/6 (H-2b) mice were from Clea Japan (Tokyo). HLA24^b-Tg was from SLC Japan (Gotoh et al. 2002). Mice were maintained in the Hokkaido University Animal Facility (Sapporo, Japan) in specific pathogen-free conditions. All experiments used mice that were 8–12 weeks old at the time of first procedure. All mice were used according to the guidelines of the institutional animal care and use committee of Hokkaido University, which approved this study (ID number: 08-0243, "Analysis of immune modulation by toll-like receptors").

Reagents, antibodies and cells

PolyI:C and $OVA_{323-339}$ peptide (ISQAVHAAHAEINEAGR) were from Sigma. $OVA_{257-264}$ peptide (SIINFEKL: SL8), OVA (H2 K^b-SL8), HLA-A*2402 survivin-2B and HIV tetramer were from MBL. SVN2B peptide (AYACNTSTL) and HLA-A*2402/2B peptide-restricted human T cell clones (Idenoue et al. 2005) were kindly provided by Dr. Noriyuki Sato (Department of Pathology, School of Medicine, Sapporo Medical University). Human and murine-specific helper peptides (Charalambous et al. 2006) $MmSVN_{13-27}$ (YLKNYRIATFKNWPF) and Hs SVN_{13-27} (FLKDHRISTFKNWPF) and the common helper peptide Hs/Mm SVN_{53-67} (DLAQCFFCFKELEGW), were synthesized by Biologica Co. Ltd (Nagoya). Peptide purity was >95%. To eliminate lipopolysaccharide contamination, all peptides were treated with 200 μg/ml polymixin B (Sigma) for 30 min at 37 °C before use (Nishiguchi et al. 2001). Anti-CD3ε (145-2C11), anti-CD8α (53-6.7) and anti-IFNγ (XMG1.2) antibodys (Abs) were from BioLegend. Anti-CD4 Ab (L3T4) was from eBiosciences and ViaProbe was from BD Biosciences. Dendritic cells were prepared from spleens of mice as described previously (Azuma et al., 2012).

Antigen-specific T cell expansion in vivo

HLA24^b Tg mice (Gotoh et al. 2002) were subcutaneously immunized with 100 μg of each antigen and 100 μg poly I:C once a week for 4 weeks. After 7 days from the last immunization, spleens were extracted, homogenized and stained with FITC-CD8α and PE-OVA (Azuma et al. 2012) or PE-SVN2B tetramer for detecting antigen-specific CD8$^+$ T cells (Tsuruma et al. 2008). For intracellular cytokine detection, splenocytes were cultured with 100 nM SL8 or survivin 2B peptide for 6 h with 10 μg/ml brefeldin A (Sigma–Aldrich) added in the last 4 h. For intracellular cytokine detection of antigen-specific CD4$^+$ T cells, splenocytes were cultured with 100 nM $OVA_{323-339}$ peptide or SVN helper peptide for 6 h with 10 μg/ml brefeldin A (Sigma–Aldrich) added in the last 5 h. Cells were stained with PE-anti-CD8α/FITC-anti-CD3ε for CD8$^+$ T cells or PE-anti-CD4/FITC-anti-CD3ε for CD4$^+$ T cells. After cell-surface staining, cells were fixed and permeabilized with Cytofix/Cytoperm (BD Biosciences) according to the manufacturer's instruction. Fixed and permeabilized cells were stained with APC-anti-IFN-γ. Stained cells were analyzed with FACSCalibur (BD Biosciences) and FlowJo software (Tree Star) (Azuma et al. 2012).

ELISA

Sera were collected from immunized mice once a week for 4 weeks and 96-well plates were coated with 10 μg/ml OVA, MmSVN2B and HsSVN2B in ELISA/ELISPOT coating buffer (eBioscience) and incubated overnight at 4 °C. ELISA diluent solution (eBioscience) was used for blocking and antibody dilution. PBS with 0.05% Tween 20 was used for washes. Anti-OVA or anti-SVN in sera was assessed by ELISA using antiserum for IgG2a/b and IgG1 diluted 1000-fold and 10,000-fold and incubated for 2 h at room temperature. After washing, isotype IgGs were detected using goat anti-mouse total IgG, IgG1, or IgG2a conjugated to HRP (Southern Biotechnology Associates). After washing, plates were stained with 1XTMB ELISA substrate solution (eBioscience) and reactions stopped with 2 N H_2SO_4 before measuring absorbance.

Statistical analyses

For comparison of two groups, *P*-values were calculated with a Student's *t*-test. For comparison of multiple groups, P-values were calculated with one-way analysis of variance (ANOVA) with Bonferroni's test. Error bars are SD or SEM between samples.

Results

Origin of human SVN exon 2B

The HsSVN gene has four conserved and two cryptic exons (Mahotka et al. 1999). The authentic HsSVN gene encode 142 amino acids in exons 1–4. On the other hand, the HsSVN2B product is 165 amino acids encoded by exons 1, 2, 2B, 3 and 4. Exon 2B is hidden within intron 2, which is spliced into mature HsSVN2B mRNA in-frame between exons 2 and 3 (Mahotka et al. 1999). Exon 2B is followed by the GT-AG role and expressed in many tumor cells and tumor cell lines, suggesting that splicing predominantly occurs in malignantly transformed cells (Mahotka et al. 2002). According to the Ensembl database, HsSVN intron 2 had two Alu sequences (Fig. 1A), and exon 2B resulted from the second Alu. In contrast, the MmSVN gene had four exons separated by three introns with no Alu sequence in intron 2; instead, MmSVN had several SINE sequences characteristic of rodents in intron 2 (Fig. 1A). Although the exon sequences were conserved in human and mouse SVNs, two intron sequences diverged between human and mouse (Fig. 1A). These results suggested that integration of exon 2B was evolutionarily new and formed after an Alu insertion. Although the SVN gene is conserved in yeast and humans, exon 2B was established after the divergence of human and mouse.

We used RT-PCR to investigate transcripts resulting from splicing other exons around exon 2 into the MmSVN mRNA. Results of mRNAs from mouse organs and cell lines are in Fig. 2B. The results suggested that no alternative exons around exon 2 in the MmSVN gene. We detected a ~200 bp product in most organs and cell lines tested (Fig. 2B), but this was not an MmSVN transcript.

Generation of a mmSVN2B construct

A SVN2B peptide derived from the HsSVN2B gene that contained the exon 2B sequence was recognized by CTLs in cancer patients (Hirohashi et al. 2002; Tsuruma et al. 2008; Honma et al. 2009) and a CTL clone was established from patients (Idenoue et al. 2005). We artificially constructed an MmSVN2B with a xenogeneic human exon 2B inserted into the boundary between exon 2 and 3 of SVN (Fig. 2A and B). Prominent amino acid substitutions between MmSVN2B and HsSVN2B were concentrated in the N-terminal region encoded by exon 1 (Fig. 2B), and a CD4 epitope is in this region (Li 2005; Mahotka et al. 2002). In an earlier paper, this $HsSVN_{13-27}$ region, but not $MmSVN_{13-27}$, was an effective CD4 epitope that promoted $HsSVN_{13-27}$-specific CD4$^+$ T cell proliferation

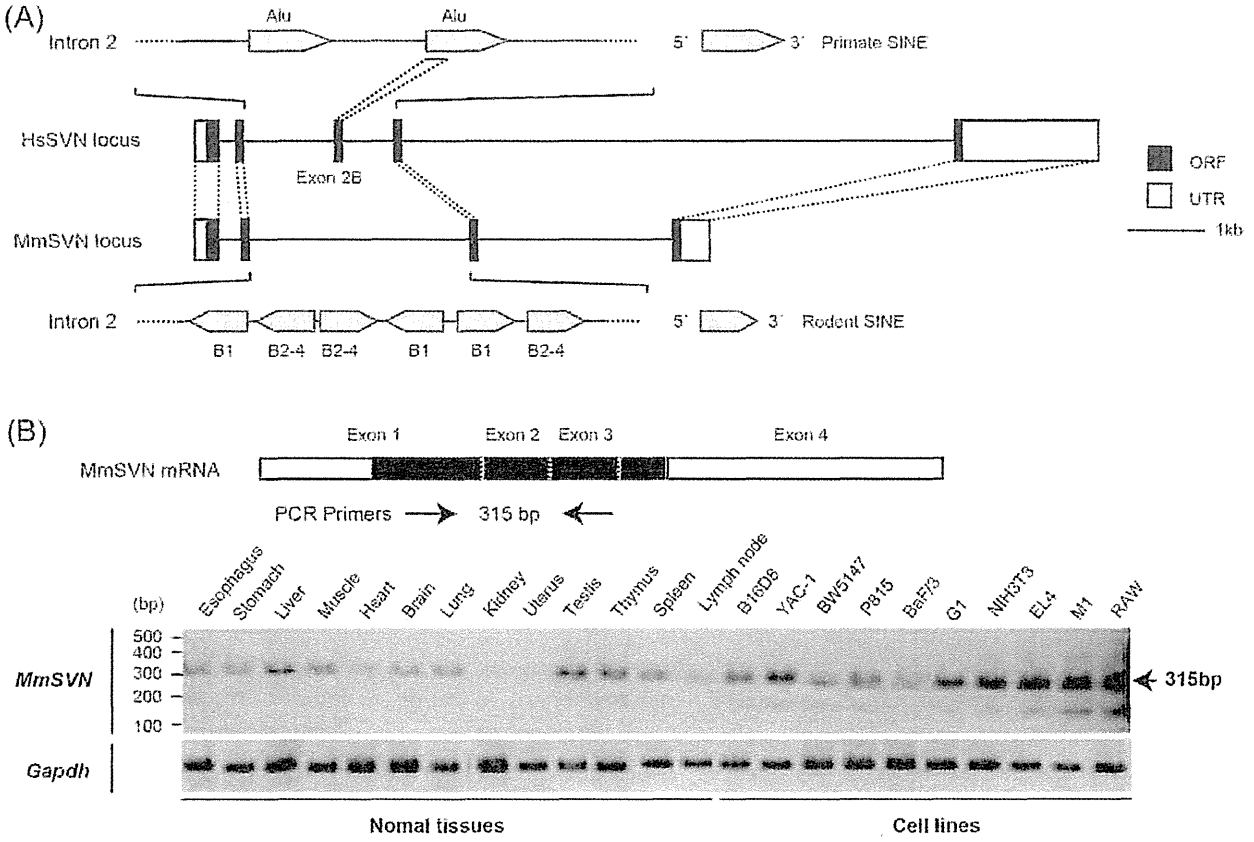

Fig. 1. Genome structure and expression of human and murine SVN gene. (A) Comparison of human and murine survivin gene structure. Survivin gene structures were defined by the Ensembl genome browser. Primate and rodent SINEs were predicted using Repeat Masker program. Filled boxes, coding regions; open boxes, 5′- and 3′-untranslated regions. (B) Structure of murine survivin transcript and RT-PCR analysis of organs and cell lines. Arrows, survivin-detecting PCR primers.

Fig. 2. Structure and purification of chimeric MmSVN2B protein. (A) Strategy for constructing chimeric MmSVN2B protein. Human exon 2B was inserted into MmSVN by PCR. (B) Alignment of murine and human SVN sequences. Black shaded area, residues conserved between human and murine SVN; Hs, human; Mm mouse. *, $MmSVN_{13-27}$/$HsSVN_{13-27}$ peptide; +, Hs/Mm SVN_{53-67} peptide; #, SVN2B peptide. (C) Purification of N-His-tagged MmSVN2B and HsSVN2B proteins. N-His-tagged SVN proteins were purified using a Profinia protein purification system from BL21 (DE3) competent cells. Purified SVN protein buffer was sequentially exchanged to PBS containing 2 M urea.

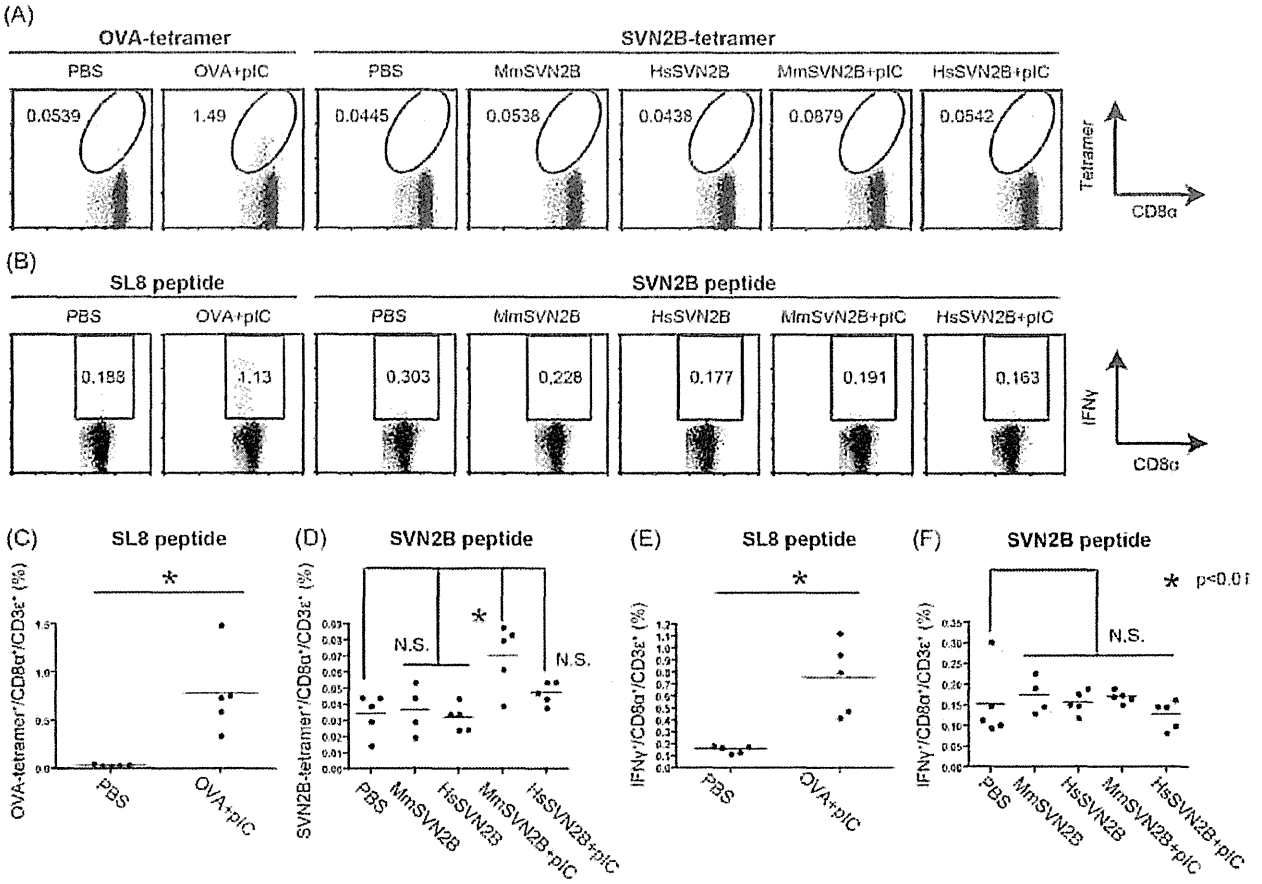

Fig. 3. Expansion of OVA and SVN-specific CD8⁺ T cells. (A) HLA24^b-Tg mice were immunized with 100 μg antigen and 100 μg poly I:C once a week for 4 weeks. After 7 days from the last immunization, spleens were homogenized and stained with FITC-CD8α and PE-OVA or PE-survivin tetramer to detect antigen-specific CD8⁺ T cells. (B) Splenocytes were cultured *in vitro* in the presence of SL8 or SVN2B peptides for 6 h and IFN-γ production was measured by FACS. (C, D) Average percentages of OVA-positive and SVN2B-tetramer positive CD8⁺ T cells shown in (A). (E, F) Average percentages of IFN-γ producing CD8⁺ T cells specifically in response to SL8 or SVN2B peptide in (B). *$p < 0.01$.

(Charalambous et al. 2006). His-tagged MmSVN2B and HsSVN2B proteins were purified and used as Ags (Fig. 2C).

CD4⁺ and CD8⁺ T cells that react to MmSVN2B plus polyI:C

We examined the ability of MmSVN2B to induce IFN-γ and CD8⁺ T cell proliferation by immunizing HLA24^b-Tg mice with MmSVN2B or HsSVN2B with or without polyI:C (Fig. 3). SVN2B-specific CTLs were probed by SVN2B-tetramer (Fig. 3A) and IFN-γ staining (Fig. 3B). SVN2B-specific human CD8⁺ T cells were detected with SVN2B-tetramer (Fig. S1), which enabled us to search for SVN2B-specific CTLs in HLA24^b-Tg mice (Idenoue et al. 2005). Expression of CD40 was up-regulated in CD8α⁺ conventional DCs to a similar extent with MmSVN2B or HsSVN2B (Fig. S2), consistent with a report on CD40 that promotes cross-priming by Ahonen et al. (J Exp Med, 2004). OVA and polyI:C were used as positive controls (Fig. 3A, B left panels), and SL8 (SIINFEKL)-specific CTLs were monitored with OVA tetramer (Azuma et al. 2012). Both OVA-tetramer-positive and IFN-γ-producing CD8⁺ T cells were detected in mice immunized with OVA and polyI:C (Fig. 3C, E). Without polyI:C stimulation, only small number of OVA-tetramer-positive cells were upregulated compared to controls (Azuma et al. 2012; Azuma & Seya unpublished data).

When HLA24^b-Tg mice were immunized with MmSVN2B or HsSVN2B without polyI:C, no significant induction of SVN2B-tetramer-positive (Fig. 3D) or IFN-γ-inducing cells was observed (Fig. 3F). When polyI:C was included, only a small increase in SVN2B-tetramer-positive cells was detected in mice given MmSVN + polyI:C with no significant increase in IFN-γ (Fig. 3F). Mice receiving HsSVN + polyI:C (Fig. 3D) or polyI:C alone (not shown) showed no significant increase in SVN2B-specific CD8⁺ T cells. Consistent with the lack of tetramer-positive CTL induction, MmSVN2B treatment failed to regress MmSVN2B-transfected tumor cells implanted into HLA24^b-Tg mice. In EG7 tumor-bearing mice, administration of polyI:C alone (without Ag) induces tumor-growth retardation due to the contribution of endogenous Ag (Azuma et al. 2012), but in this case with tumor-unloaded mice polyI:C exhibited no tumor-regressing activity (data not shown), possibly due to the lack of Ag.

Next, we determined the amounts of CD4⁺ T cells that reacted with MmSVN2B. The positive control group received OVA Ag and polyI:C (Fig. 4A, B). The negative control group received PBS without Ag and polyI:C, but basal frequencies of IFN-γ-producing CD4⁺ T cells were detected in this group even in the absence of polyI:C or Ag (Fig. 4). When MmSVN2B or HsSVN2B only was used to immunize mice, no significant response was seen in CD4⁺ T cells compared to PBS controls (Fig. 4A, C–E). When polyI:C was included, IFN-γ-producing CD4⁺ T cells restimulated with Hs/MmSVN$_{53-67}$ peptide increased significantly in mice that received MmSVN and HsSVN (Fig. 4C, D). The sequence of MmSVN$_{53-67}$ was identical to the sequence of HsSVN$_{53-67}$ (Fig. 2B). However, we did not detect a significant increase in IFN-γ-producing CD4⁺ T cells in mice